NASA/TP—2006–214711

An Examination of Selected Geomagnetic Indices in Relation to the Sunspot Cycle

Robert M. Wilson and David H. Hathaway
Marshall Space Flight Center, Marshall Space Flight Center, Alabama

December 2006

The NASA STI Program…in Profile

Since its founding, NASA has been dedicated to the advancement of aeronautics and space science. The NASA Scientific and Technical Information (STI) Program Office plays a key part in helping NASA maintain this important role.

The NASA STI program operates under the auspices of the Agency Chief Information Officer. It collects, organizes, provides for archiving, and disseminates NASA's STI. The NASA STI program provides access to the NASA Aeronautics and Space Database and its public interface, the NASA Technical Report Server, thus providing one of the largest collections of aeronautical and space science STI in the world. Results are published in both non-NASA channels and by NASA in the NASA STI Report Series, which includes the following report types:

- TECHNICAL PUBLICATION. Reports of completed research or a major significant phase of research that present the results of NASA programs and include extensive data or theoretical analysis. Includes compilations of significant scientific and technical data and information deemed to be of continuing reference value. NASA's counterpart of peer-reviewed formal professional papers but has less stringent limitations on manuscript length and extent of graphic presentations.

- TECHNICAL MEMORANDUM. Scientific and technical findings that are preliminary or of specialized interest, e.g., quick release reports, working papers, and bibliographies that contain minimal annotation. Does not contain extensive analysis.

- CONTRACTOR REPORT. Scientific and technical findings by NASA-sponsored contractors and grantees.

- CONFERENCE PUBLICATION. Collected papers from scientific and technical conferences, symposia, seminars, or other meetings sponsored or cosponsored by NASA.

- SPECIAL PUBLICATION. Scientific, technical, or historical information from NASA programs, projects, and missions, often concerned with subjects having substantial public interest.

- TECHNICAL TRANSLATION. English-language translations of foreign scientific and technical material pertinent to NASA's mission.

Specialized services also include creating custom thesauri, building customized databases, and organizing and publishing research results.

For more information about the NASA STI program, see the following:

- Access the NASA STI program home page at <http://www.sti.nasa.gov>

- E-mail your question via the Internet to <help@sti.nasa.gov>

- Fax your question to the NASA STI Help Desk at 301–621–0134

- Phone the NASA STI Help Desk at 301–621–0390

- Write to:
  NASA STI Help Desk
  NASA Center for AeroSpace Information
  7115 Standard Drive
  Hanover, MD 21076–1320

NASA/TP—2006–214711

An Examination of Selected Geomagnetic Indices in Relation to the Sunspot Cycle

Robert M. Wilson and David H. Hathaway
Marshall Space Flight Center, Marshall Space Flight Center, Alabama

National Aeronautics and
Space Administration

Marshall Space Flight Center • MSFC, Alabama 35812

December 2006

Available from:

NASA Center for AeroSpace Information
7115 Standard Drive
Hanover, MD 21076–1320
301–621–0390

This report is also available in electronic form at
<https://www2.sti.nasa.gov>

TABLE OF CONTENTS

LIST OF FIGURES

LIST OF FIGURES (Continued)

LIST OF TABLES

LIST OF ACRONYMS AND NOMENCLATURE

aa	antipodal geomagnetic index
$<aa>$	cyclic average of aa
aa_{90}	90-percent interval for aa
$<aa>_{90}$	90-percent interval for $<aa>$
aa (adjusted)	aa adjusted value, equal to aa (observed) + 3 for aa values prior to 1957
$<aa>$ (adjusted)	cyclic average of adjusted aa
$aa_{\mathrm{CHL/FRD}}$	the proxy aa index based on two 3-hr intervals (0–6 UT) from Cheltenham and Fredericksburg
aa_I	interplanetary component of aa ($=aa-aa_R$)
aa_I (adjusted)	interplanetary component of adjusted aa
aa_I (adjusted) $\max_2$	maximum value of 2-yr moving average of aa_I (adjusted)
aa_Imax	maximum value of aa_I
$aa_I\max_2$	maximum value of 2-yr moving average of aa_I
aa_Imax (last)	maximum value of aa_I (last), the last peak in the decline of the cycle
aamin	minimum yearly average aa value in the vicinity of cycle minimum
aamin (adjusted)	minimum yearly average adjusted aa value
aa_R	sunspot cycle component of aa
Ap	daily equivalent planetary amplitude geomagnetic index
$<Ap>$	cyclic average of Ap
Ap (adjusted)	adjusted Ap
Ap_I	interplanetary component of Ap ($=Ap-Ap_R$)

LIST OF ACRONYMS AND NOMENCLATURE (Continued)

$Ap\text{max}$	maximum value of Ap
$Ap_I\text{max}$	maximum value of Ap_I
$Ap_I\text{max}_2$	maximum value of 2-yr moving average of Ap_I
$Ap_I\text{max}\,(\text{last})$	maximum value of Ap_I (last), the last peak in the decline of the cycle
$Ap\text{min}$	minimum yearly average Ap value
Ap_R	sunspot cycle component of Ap
bv	bivariate
cl	confidence level
$d\text{max}$	maximum daily value of R during year
$E(aa\text{min})$	epoch of aamin for cycle n
$E(aa\text{min})_{n+1}$	epoch of aamin for cycle $n+1$
$E(aa_I\text{max})$	epoch of aa_Imax
$E(aa_I\text{max}\,(\text{last}))$	epoch of $aa_I\text{max}\,(\text{last})$
$E(Ap\text{max})$	epoch of Apmax
$E((Ap\text{max})\text{min})_{n+1}$	epoch of (Apmax)min for cycle $n+1$
$E(Ap\text{min})_{n+1}$	epoch of Apmin for cycle $n+1$
$E(\text{NDDmin})_{n+1}$	epoch of NDDmin for cycle $n+1$
$E(\text{NSSCmin})_{n+1}$	epoch of NSSCmin for cycle $n+1$
$E(R\text{max})$	epoch of sunspot maximum amplitude
$E(R\text{max})_{n+1}$	epoch of sunspot maximum amplitude for cycle $n+1$
$E(R\text{min})$	epoch of sunspot minimum amplitude
$E(R\text{min})_{n+1}$	epoch of sunspot minimum amplitude for cycle $n+1$

LIST OF ACRONYMS AND NOMENCLATURE (Continued)

IHV	Inter-Hour Variability (geomagnetic index)
K	geomagnetic index scaled semilogarithmically
n	sunspot cycle number; sample size
ND ($Ap \geq 100$)	number of days when $Ap \geq 100$
ND ($Ap \geq 200$)	number of days when $Ap \geq 200$
NDD	number of disturbed days (days when $Ap \geq 25$)
<NDD>	cyclic average of NDD
NDD_I	interplanetary component of NDD ($= NDD - NDD_R$)
$NDD_I max$	maximum value of NDD_I
$NDD_I max_2$	maximum value of 2-yr moving average of NDD_I
$NDD_I max$ (last)	maximum value of NDD_I(last)
NDDmin	minimum yearly NDD
NDD_R	sunspot cycle component of NDD
NH	Northern Hemisphere
NSD	number of spotless days
NSSC	number of sudden storm commencements
<NSSC>	cyclic average of NSSC
$<NSSC>_{90}$	90-percent interval of <NSSC>
R	sunspot number
$<R>$	cyclic average of R
R_{90}	90-percent interval of R
$<R>_{90}$	90-percent interval of $<R>$
r	coefficient of correlation
r^2	coefficient of determination

LIST OF ACRONYMS AND NOMENCLATURE (Continued)

RM	maximum amplitude (smoothed monthly mean sunspot number)
RM_{90}	90-percent interval for RM
Rm	minimum amplitude (smoothed monthly mean sunspot number)
Rm_{90}	90-percent interval for Rm
Rmax	maximum yearly average sunspot number (maximum amplitude)
$R\text{max}_2$	maximum amplitude of 2-yr moving average of R
$R\text{max}_{90}$	90-percent interval for Rmax
Rmin	minimum yearly average sunspot number (minimum amplitude)
$R\text{min}_2$	minimum amplitude of 2-yr moving average of R
$R\text{min}_{90}$	90-percent interval for Rmin
$R_{\text{Y.12}}$	correlation coefficient for bivariate fit
sd	standard deviation
se	standard error of estimate
SH	Southern Hemisphere
$S_{\text{Y.12}}$	standard error of estimate for bivariate fit
UT	universal time
x	independent variable
y	dependent variable
$\Delta_{1, 2, 3, 4, 5}$	differences 1, 2, 3, 4, 5
ΣNDD	sum of NDD over solar cycle
ΣNSSC	sum of NSSC over solar cycle
ΣNSSC_{90}	90-percent interval for <NSSC>

TECHNICAL PUBLICATION

AN EXAMINATION OF SELECTED GEOMAGNETIC INDICES IN RELATION TO THE SUNSPOT CYCLE

1. INTRODUCTION

Over the years, a number of geomagnetic indices have been devised to describe the variation of the geomagnetic field in response to the changing conditions of the solar wind at Earth.[1,2] A few of these indices, in fact, have been shown to reliably predict the strength of the following sunspot cycle several years in advance.[3–14] It is this aspect that will be examined more closely in this Technical Publication.

This study is divided into seven results sections. Section 2.1 examines the observed yearly average values of the *aa* and *Ap* geomagnetic indices, as well as the number of disturbed days (NDD), defined as those days when the *Ap* index equals or exceeds 25, all in relation to annual sunspot number (*R*). The *aa* index was introduced by Mayaud in the early 1970s[15,16] and is defined as the average of 3-hr *K* indices converted to the amplitude of the field at two nearly antipodal observatories (in England and Australia). The *aa* index, as derived by Mayaud, is available from 1868 to the present. Although Nevanlinna and Kataja[17] have provided an extension for the *aa* index back to 1844 using Helsinki magnetic records, these extended values have not been used in the present study. *Ap*, or the daily equivalent planetary amplitude, is a daily index of geomagnetic activity that is determined using a linear scale rather than the quasi-logarithmic scale of the *K* indices. Values for it and NDD are available from 1932 to the present. (Yearly values of *R*, *aa*, and *Ap* can be found online at ftp://ftp.ngdc.noaa.gov/STP/.[18])

Section 2.2 examines the effects of suggested changes to the observed *aa* record. Svalgaard, Cliver, and Le Sager[19] derived a new geomagnetic index called the Inter-Hour Variability (IHV) index for investigations of the long-term variability of the solar wind-magnetosphere system and used it to reconstruct the observed *aa* record. For the interval 1957–2000, they found yearly averages of their proxy *aa* index (based on observations at Cheltenham/Fredericksburg during the two 3-hr periods between 0 and 6 hr UT) and the IHV index to be virtually the same, while for the interval preceding 1957, there was considerable difference between the indices. Hence, they concluded that values of the observed *aa* index prior to 1957 might be inaccurate.

Section 2.3 examines annual minimum values of *aa*, *Ap,* and NDD (*aa*min, *Ap*min, and NDDmin, respectively) for each cycle in relation to *R*max (the annual maximum amplitude of the sunspot cycle), both as single-variate and bivariate fits (the latter fit also using *R*min, the annual minimum amplitude of the sunspot cycle). Single-variate and bivariate fits previously have been shown to reliably predict the size of the ongoing sunspot cycle some 2 to 3 years in advance.[5]

Section 2.4 examines cyclic averages (minimum-to-minimum based on *R*) of *aa*, *Ap*, NDD, and NSSC (the number of sudden storm commencements), denoted <*aa*>, <*Ap*>, <NDD>, and <NSSC>, respectively, and the cyclic sums (the total number recorded over the sunspot cycle) of NDD and NSSC, denoted ΣNDD and ΣNSSC, respectively, all in relation to the cyclic average of *R*, denoted <*R*>, and *R*min and *R*max.

Section 2.5 examines *Ap*max and the number of days when *Ap* equals or exceeds 100 and 200, denoted ND ($Ap \geq 100$) and ND ($Ap \geq 200$), respectively.

Section 2.6 identifies single-variate and bivariate regressions of *Ap*, NDD, and *Ap*max against *aa* and *aa* and *R*, respectively, for the interval of 1932–2005. These regressions are then used to provide estimates of *Ap*, NDD, and *Ap*max prior to 1932.

Section 2.7 looks at epoch analyses of sunspot number and the various geomagnetic parameters (*aa*, *Ap*, NDD, *Ap*max, and NSSC) relative to *E*(*R*max) and *E*(*R*min) to determine when onset for cycle 24 should be expected.

2. RESULTS AND DISCUSSION

2.1 Geomagnetic Indices: *aa*, *Ap*, and NDD

Figure 1 displays the annual variation of sunspot number *R* in (panel (a)), *aa* (panel (b)), *Ap* (panel (c)), and NDD (panel (d)). For *R* and *aa*, values are given for 1868–2005, while for *Ap* and NDD, values are given for 1932–2005. The lower numbers refer to sunspot cycles 11–23. The thin vertical lines refer to the occurrences of the sunspot minimum year for each of the sunspot cycles.

Inspection of figure 1 reveals two important aspects of solar/geomagnetic activity: First, there has been a general rise in *R* and *aa* over the years and second, while *R* usually is single peaked, *aa* (and *Ap* and NDD) generally has two or more peaks, with the first being closely associated with the rising/maximum phase of the sunspot cycle and the other(s) occurring during the declining portion of the sunspot cycle, often occurring just prior to the onset of the new cycle. Hathaway, Wilson, and Reichmann[20] previously have shown that the secular trend in *R* is long-term, extending from the Maunder minimum. Also, Clilverd et al.,[21] using two long-running European stations (Sodankylä and Niemegk), have reconstructed the long-term *aa* index and concluded that the trend in *aa* is real, inferring a long-term increase in solar coronal magnetic field strength. Indeed, Wilson and Hathaway[22] have reported that, on the basis of 10-yr moving averages, *R* and *aa* are highly correlated ($r = 0.933$).

In order to explain the later-occurring peaks in the *aa* index (which nearly always have been the largest of the cycle), Feynman[23] suggested that two components comprise the *aa* index—one that is in phase and correlated directly with the sunspot cycle and the other (the residual) that is out of phase and associated with interplanetary disturbances from the Sun (high-speed solar wind streams and the like[24]). Figure 2 plots *aa* versus *R* (panel (a)), *Ap* versus *R* (panel (b)), and NDD versus *R* (panel (c)). The identified lines in each panel are those that allow for a determination of the inferred sunspot cycle component for the geomagnetic indices by passing a line through the two lowest points. Hence, all geomagnetic index values lie either on or above these lines. By subtracting this component from the observed value of the geomagnetic index, one infers the value of the residual interplanetary component. (The technique employed here is slightly different from that employed in Hathaway, Wilson, and Reichmann[13] and Hathaway and Wilson.[14])

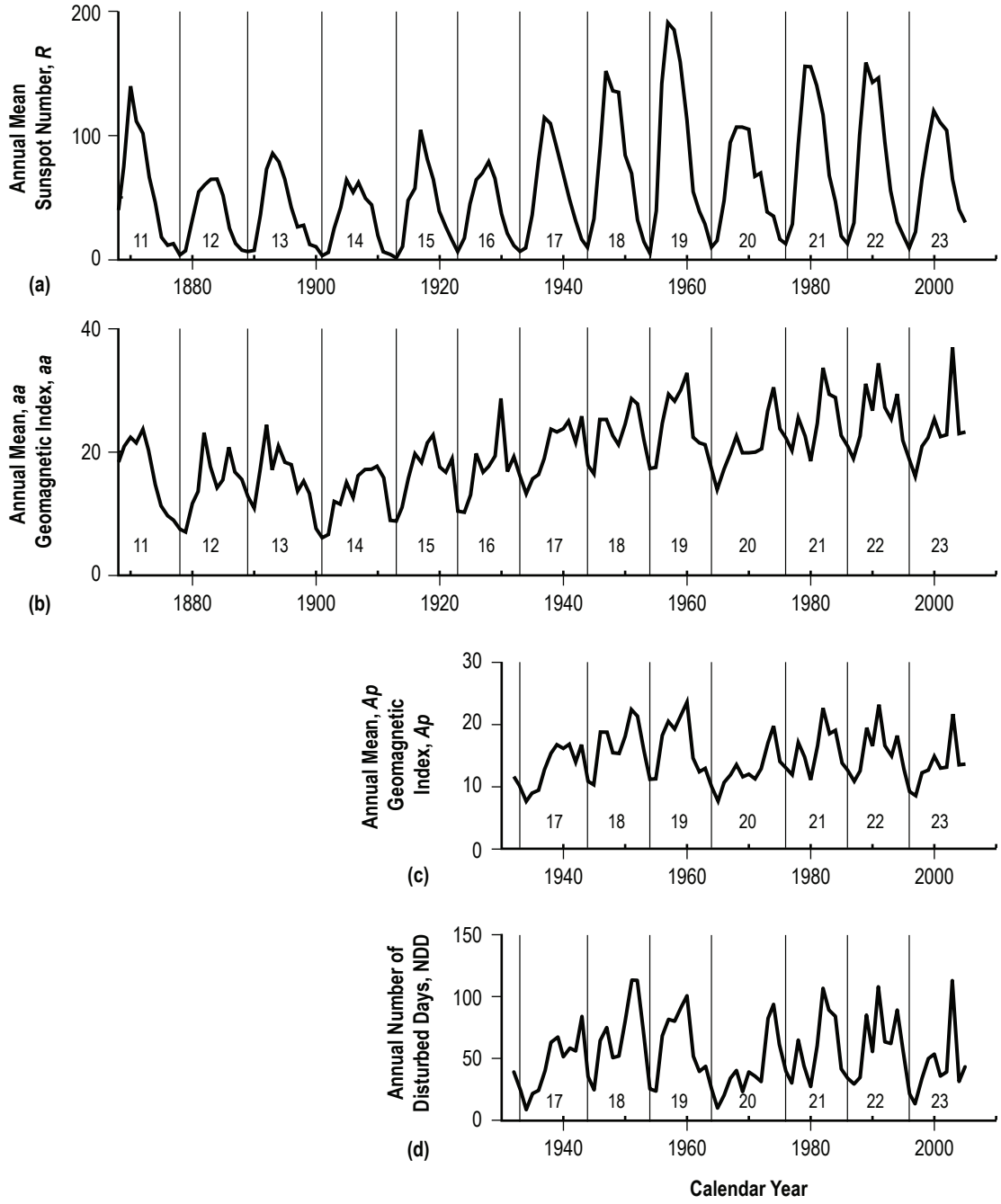

Figure 1. Variation of annual averages of sunspot number, *R* (panel (a)); *aa*-geomagnetic index, *aa* (panel (b)); *Ap*-geomagnetic index, *Ap* (panel (c)); and number of disturbed days, NDD (panel (d)). See text for details.

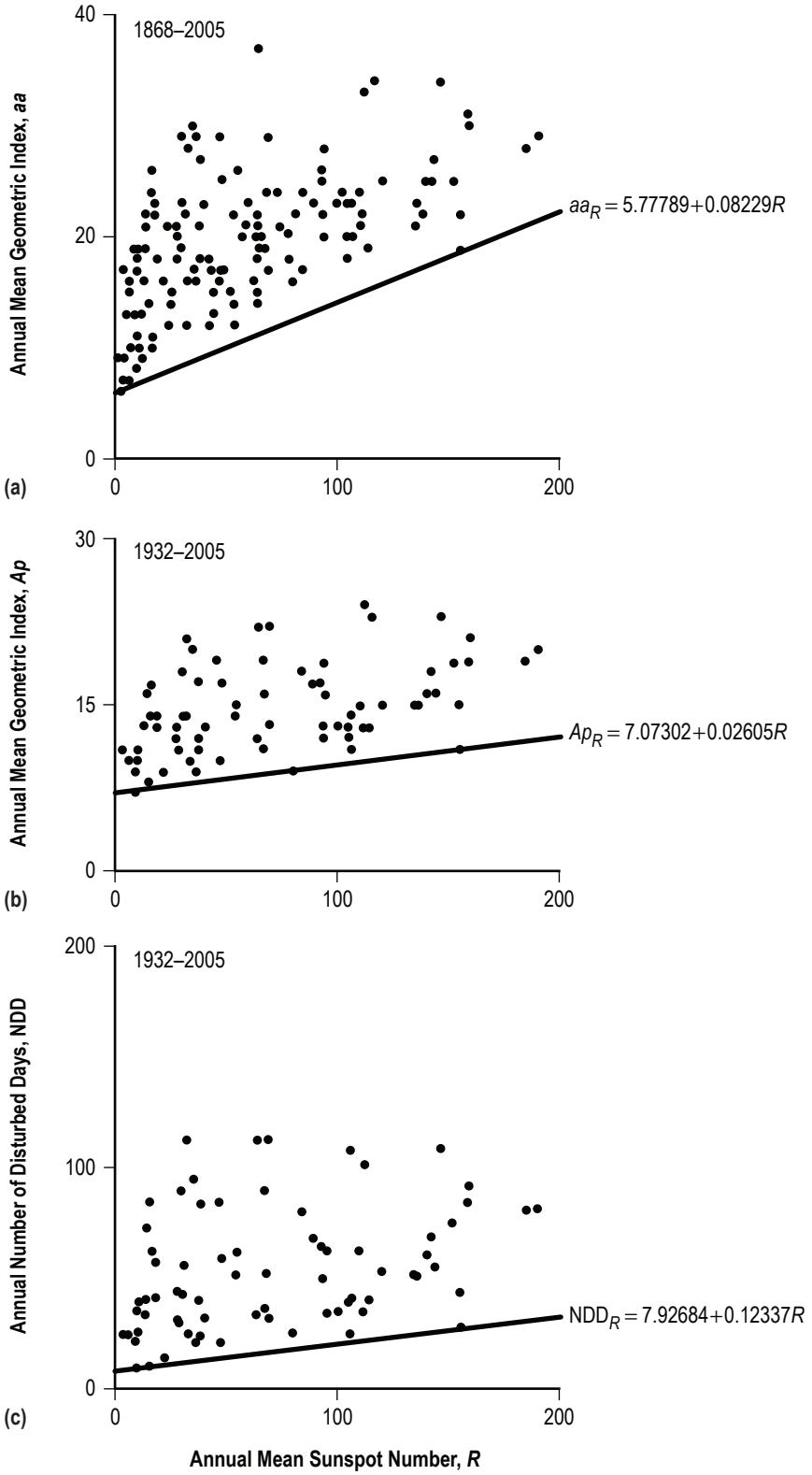

Figure 2. Scatterplots of *aa* versus *R* (panel (a)); *Ap* versus *R* (panel (b)); and NDD versus *R* (panel (c)). All values of the geomagnetic indices lie on or above the identified regression lines.

Figure 3 plots the residual interplanetary components of aa_I (panel (a)), Ap_I (panel (b)), and NDD_I (panel (c)), all plotted as the thin jagged lines. The thicker, smoother lines are 2-yr moving averages[25] of the residuals (using a weighting of 1:2:1), and, as before, the lower numbers refer to the individual sunspot cycles 11–23 and the thin vertical lines mark the occurrences of the sunspot minimum years.

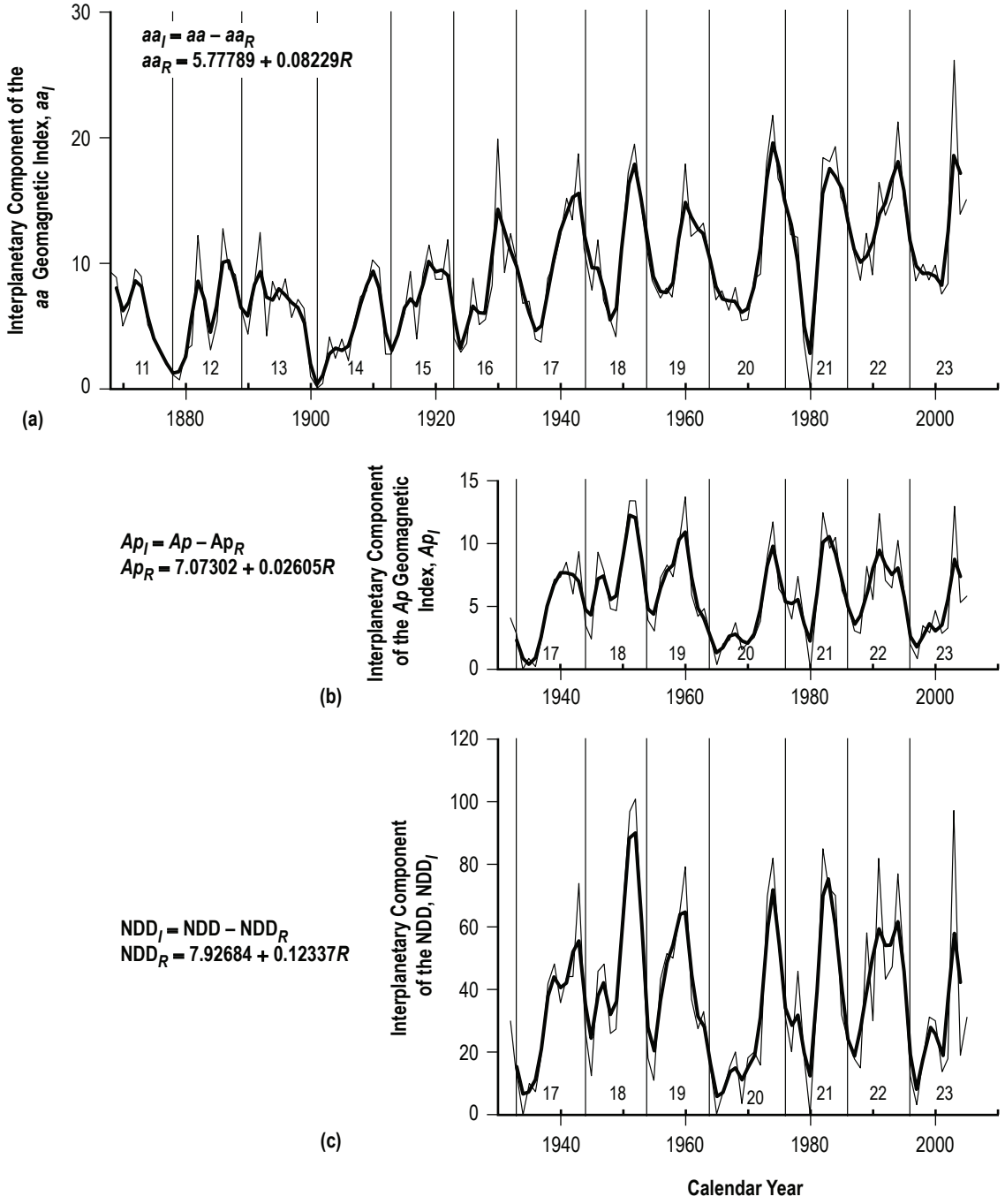

Figure 3. Variation of the interplanetary components aa_I (panel (a)); Ap_I (panel (b)); and NDD_I (panel (c)). The thick lines are 2-yr moving averages of the residual interplanetary components.

Figure 4 shows histograms marking the frequency of occurrences for the maximum amplitude of aa_I ($E(aa_I\text{max}$, panel (a)) and for the last occurrences of the local maximums of aa_I ($E(aa_I\text{max}$ (last), panel (b)), which often also turns out to be $E(aa_I\text{max})$ for most of the cycles (11, 12, 14, 15, 17, 18, 21, and 22), in years relative to the occurrences of $E(R\text{max})$. For $E(aa_I\text{max})$, two cycles (11 and 16) have $E(aa_I\text{max})$ 2 yr after $E(R\text{max})$; four cycles (12, 13, 19, and 23) have $E(aa_I\text{max})$ 3 yr after $E(R\text{max})$; five cycles (14, 15, 18, 21, and 22) have $E(aa_I\text{max})$ 5 yr after $E(R\text{max})$; and two cycles (17 and 20) have $E(aa_I\text{max})$ 6 yr after $E(R\text{max})$. For $E(aa_I\text{max}$ (last)), the bulk of the cycles (13, 14, 15, 18, 21, 22, and 23) have $E(aa_I\text{max}$ (last)) 5 yr after $E(R\text{max})$.

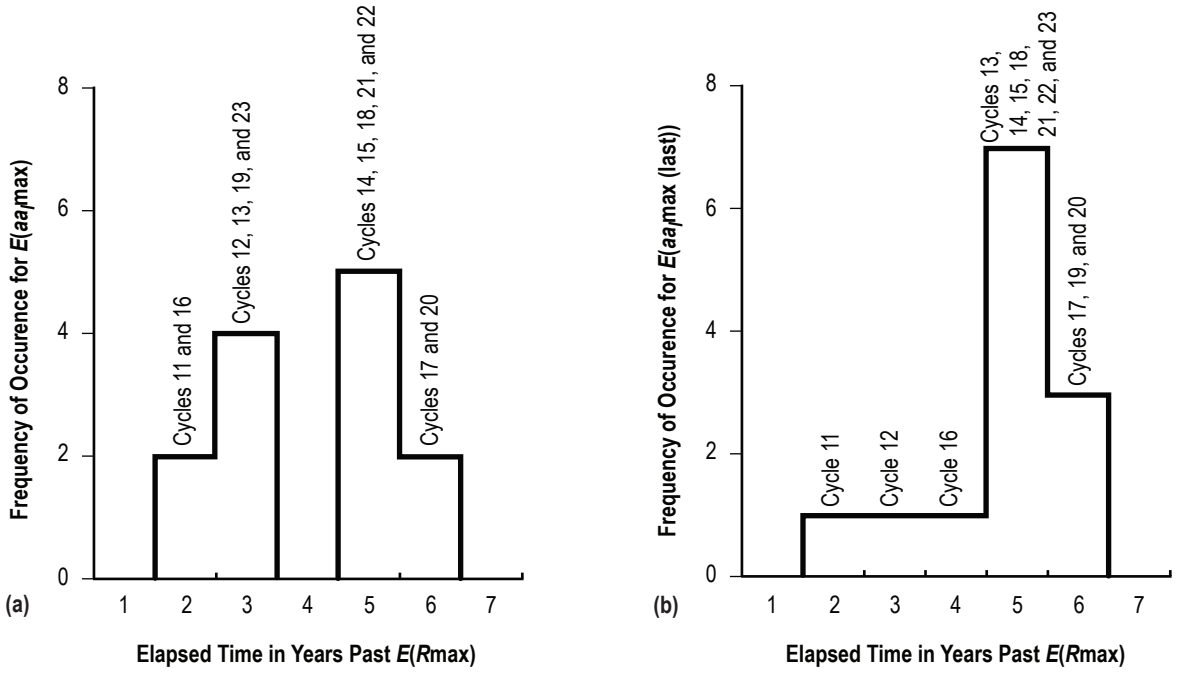

Figure 4. Histograms of the frequency of occurrences for $E(aa_I\text{max})$ (panel (a)) and $E((aa_I\text{max}$ (last)) (panel (b)), relative to the elapsed time in years from $E(R\text{max})$.

Figure 5 displays scatterplots of $R\text{min}$ (cycle $n+1$) versus $aa_I\text{max}$ (cycle n) (panel (a)); $R\text{min}$ (cycle $n+1$) versus $Ap_I\text{max}$ (cycle n) (panel (b)); $R\text{min}$ (cycle $n+1$) versus NDD_Imax (cycle n) (panel (c)); $R\text{max}$ (cycle $n+1$) versus $aa_I\text{max}$ (cycle n) (panel (d)); $R\text{max}$ (cycle $n+1$) versus $Ap_I\text{max}$ (cycle n) (panel (e)); and $R\text{max}$ (cycle $n+1$) versus NDD_Imax (cycle n) (panel (f)). In each panel, the small, downward-pointing arrow marks the parametric value for cycle 23. For panels (b), (c), (e), and (f), no statistically significant (confidence level (*cl*) ≥95 percent) linear correlation can be inferred between the parameters. For these, only the mean and standard deviation (*sd*) are shown. However, for panels (a) and (d), statistically significant positive linear correlations are inferred (those related to $aa_I\text{max}$). Thus, given $aa_I\text{max} = 26.1$ for cycle 23, one infers $R\text{min} = 13 \pm 4.9$ and $R\text{max} = 183.7 \pm 46.3$ for cycle 24, the next sunspot cycle. Both predictions are 90-percent prediction intervals so, there is only a 5-percent chance that $R\text{min}$ will be smaller than 9.1 and $R\text{max}$ will be smaller than 137.4. Likewise, there is only a 5-percent chance that $R\text{min}$ will be larger than 17.9 and $R\text{max}$ will be larger than 230.

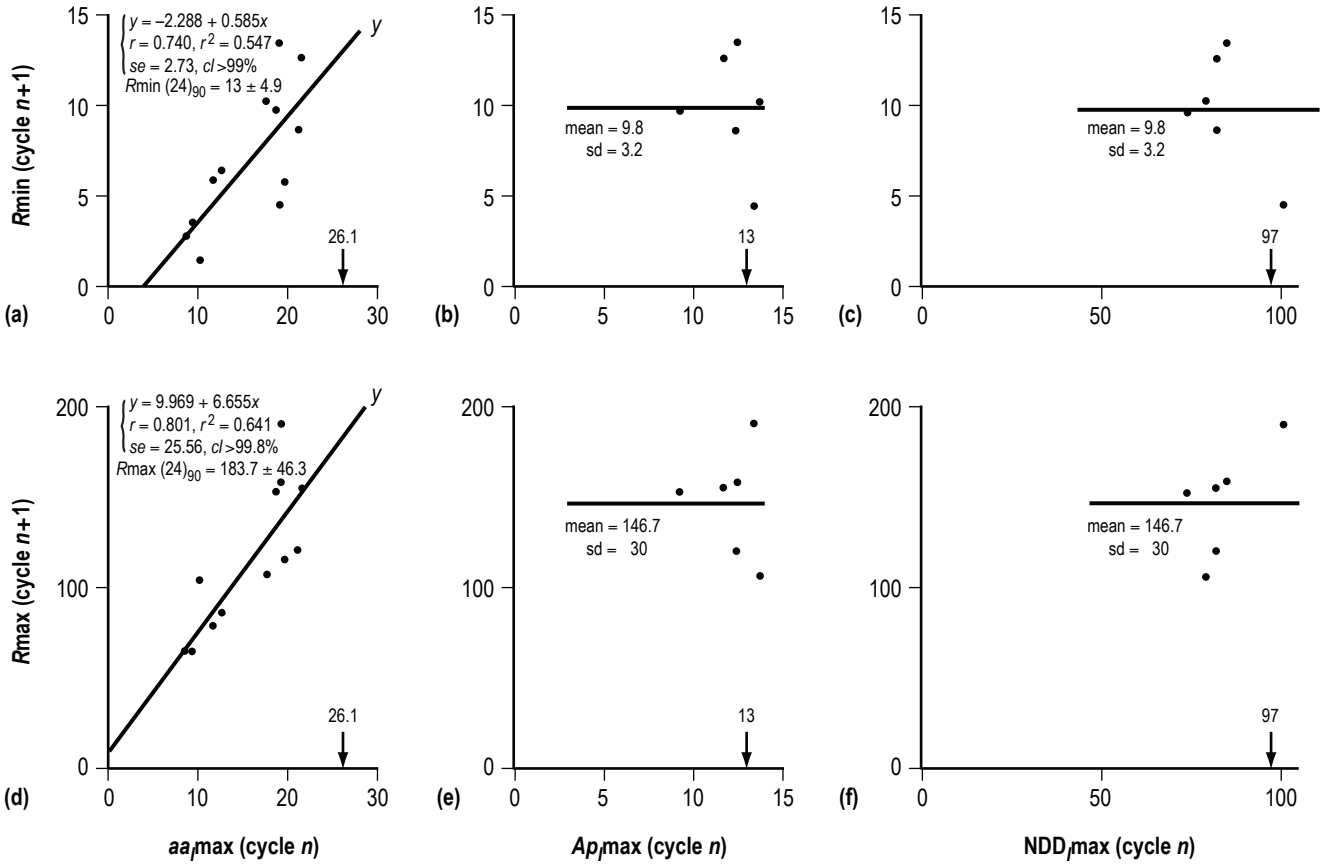

Figure 5. Scatterplots of *R*min (cycle $n+1$) versus selected maximum interplanetary components for cycle n (panels (a)–(c)) and *R*max (cycle $n+1$) versus selected maximum interplanetary components for cycle n (panels (d)–(f)). See text for detail.

Figure 6 depicts scatterplots of *R*min (cycle $n+1$) versus aa_Imax (last) (cycle n) (panel (a)); *R*min (cycle $n+1$) versus Ap_Imax (last) (cycle n) (panel (b)); *R*min (cycle $n+1$) versus NDD_Imax (last) (cycle n) (panel (c)); *R*max (cycle $n+1$) versus aa_Imax (last) (cycle n) (panel (d)); *R*max (cycle $n+1$) versus Ap_Imax (last) (cycle n) (panel (e)); and *R*max (cycle $n+1$) versus NDD_Imax (last) (cycle n) (panel (f)). For panels (b) and (c), no statistically significant linear correlation can be inferred between the parameters. For these, only the mean and *sd* are shown. For the other panels, statistically significant positive linear correlations are inferred. Thus, given aa_Imax (last) = 15 for cycle 23 (an assumed value, since the values for 2006 and 2007 are presently unknown, true also for Ap_Imax (last) and NDD_Imax (last)), one infers *R*min = 7.2 ± 5 and *R*max = 117.5 ± 41.2 for cycle 24. Also, given Ap_Imax (last) = 5.8 and NDD_Imax (last) = 31 for cycle 23, one infers *R*max = 110.1 ± 38.4 and *R*max = 96.2 ± 35.6, respectively, for cycle 24. These predictions clearly differ with the aforementioned predictions based on aa_Imax for cycle 23.

Figure 7 shows scatterplots of $R\mathrm{min}_2$ (cycle $n+1$) versus $aa_I\mathrm{max}_2$ (cycle n) (panel (a)), where the subscript 2 refers to the 2-yr moving average (shown in fig. 3 as the thicker smoother lines); $R\mathrm{min}_2$ (cycle $n+1$) versus $Ap_I\mathrm{max}_2$ (cycle n) (panel (b)); $R\mathrm{min}_2$ (cycle $n+1$) versus $\mathrm{NDD}_I\mathrm{max}_2$ (panel (c));

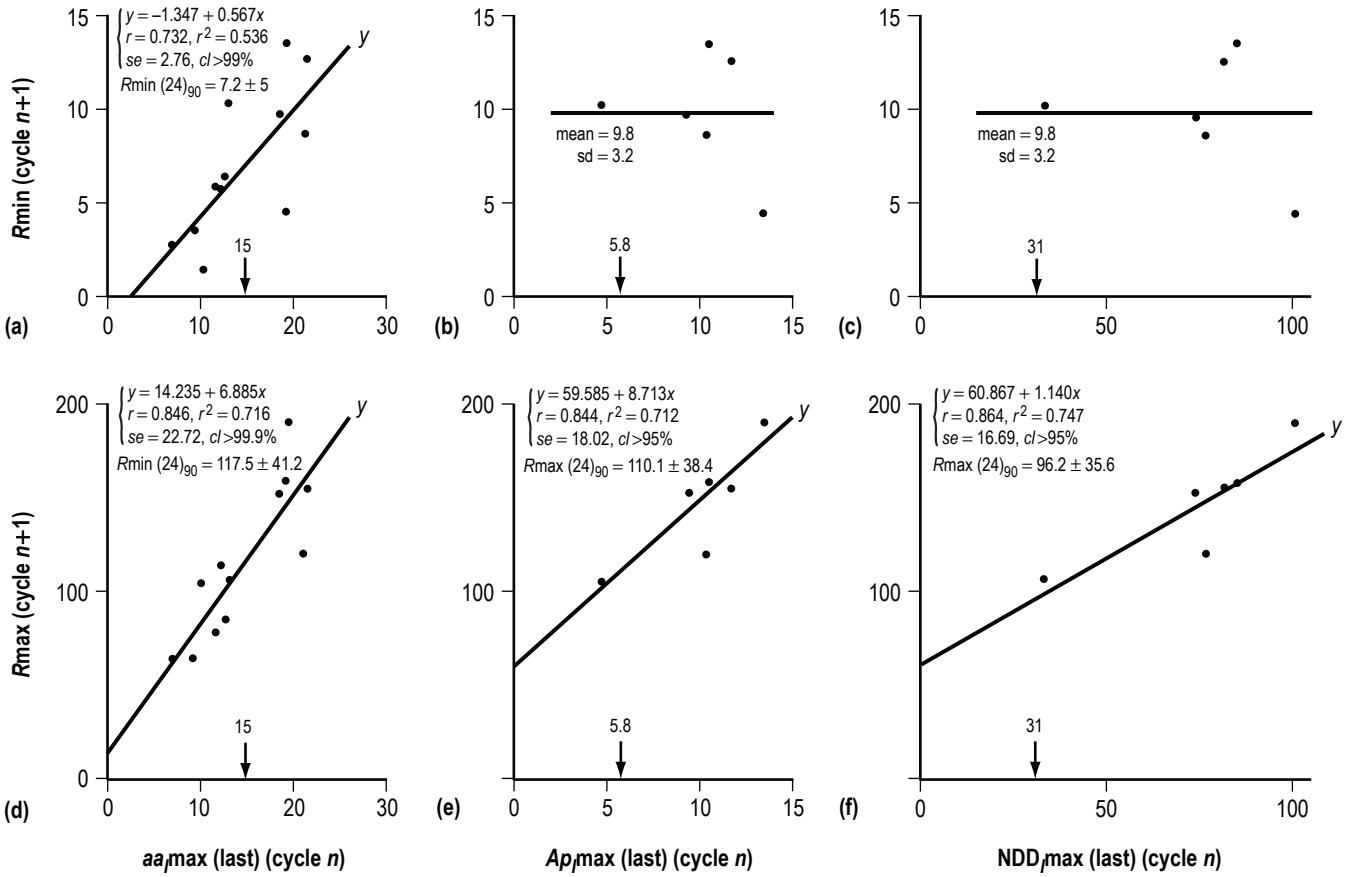

Figure 6. Scatterplots of *R*min (cycle $n+1$) versus selected last-occurring maximum interplanetary components for cycle n (panels (a)–(c)) and *R*max (cycle $n+1$) versus selected last-occurring maximum interplanetary components for cycle n (panels (d)–(f)). See text for details.

$R\max_2$ (cycle $n+1$) versus $aa_I\max_2$ (cycle n) (panel (d)); $R\max_2$ (cycle $n+1$) versus $Ap_I\max_2$ (cycle n) (panel (e)); and $R\max_2$ (cycle $n+1$) versus $\mathrm{NDD}_I\max_2$ (cycle n) (panel (f)). Only panels (a) and (d) are found to contain a statistically significant positive linear correlation, both having higher coefficients of correlation (r) and smaller standard errors (se) than for either of the unsmoothed plots (figs. 5 and 6). Thus, given $aa_I\max_2 = 18.6$ for cycle 23, one infers $R\min_2 = 16.9 \pm 4.8$ and $R\max_2 = 146.7 \pm 30.5$ for cycle 24, both predictions being 90-percent prediction intervals. Hence, there is only a 5-percent chance that cycle 24's $R\min_2$ will be smaller than 12.1 or larger than 21.7, and there is only a 5-percent chance that cycle 24's $R\max_2$ will be smaller than 116.2 or larger than 177.2. The 90-percent prediction interval for cycle 24's $R\min_2$ suggests that its *R*min (the annual average value) will be about 10.4 ± 3 and its *Rm* (12-mo moving average, or smoothed monthly mean sunspot number minimum amplitude) will be about 9.4 ± 2.9. Similarly, the 90-percent prediction interval for cycle 24's $R\max_2$ suggests that its *R*max (the annual average value) will be about 157.5 ± 31.8 and its *RM* (12-mo moving average, or smoothed monthly mean sunspot number maximum amplitude) will be about 162.9 ± 33.5. Thus, these values suggest that cycle 24's activity will be greater than average (and larger than was seen for cycle 23), similar in size to that experienced in cycles 21 and 22.[14,26,27]

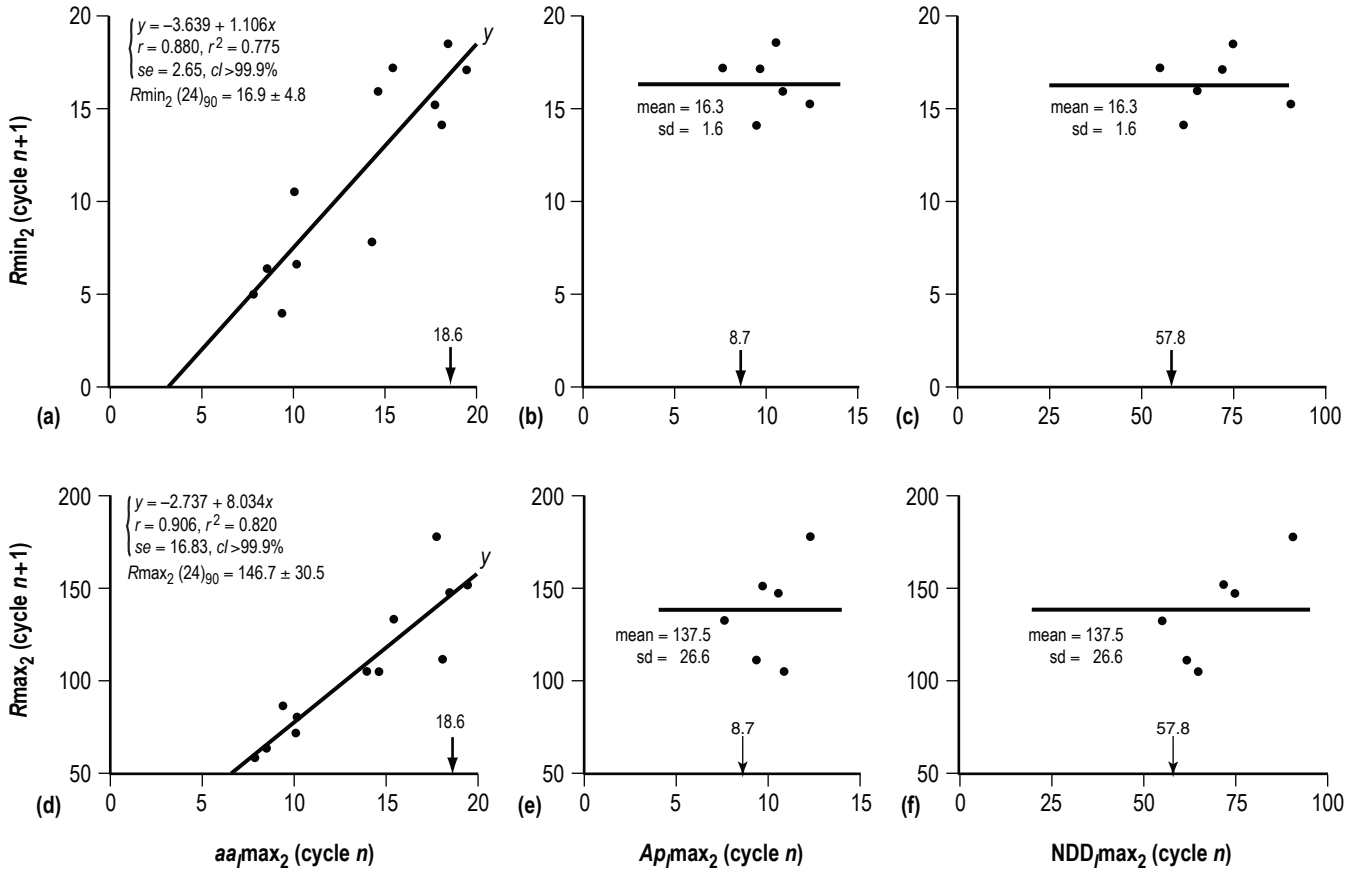

Figure 7. Scatterplots of $R\text{min}_2$ (cycle $n+1$) versus selected 2-yr moving averages of the maximum interplanetary components for cycle n (panels (a)–(c)) and $R\text{max}_2$ (cycle $n+1$) versus 2-yr moving averages of the maximum interplanetary components for cycle n (panels (d)–(f)). See text for details.

2.2 *aa* (adjusted) Geomagnetic Index

Recall from figure 1 the long-term rise in the observed *aa* index over time, which is also apparent in *R*, this indicating a strong correlation between the parameters. Indeed, as previously mentioned, Wilson and Hathaway[22] have noted that on the basis of 10-yr moving averages, *aa* and *R* are highly correlated ($r=0.933$). Also, as previously mentioned, Svalgaard, Cliver, and Le Sager[19] in their reconstruction of the observed *aa* index using the IHV index found that, for the interval of 1957–2000, both parameters are virtually identical, while for the interval preceding 1957, the reconstructed *aa* (based on the IHV index) lies above the observed *aa*. Hence, they concluded that the observed *aa* prior to 1957 might be inaccurate. (In 1957, the Northern Hemisphere (NH) magnetometer used in deriving the *aa* index was moved from Abinger, England, to its present location in Hartland, England.)

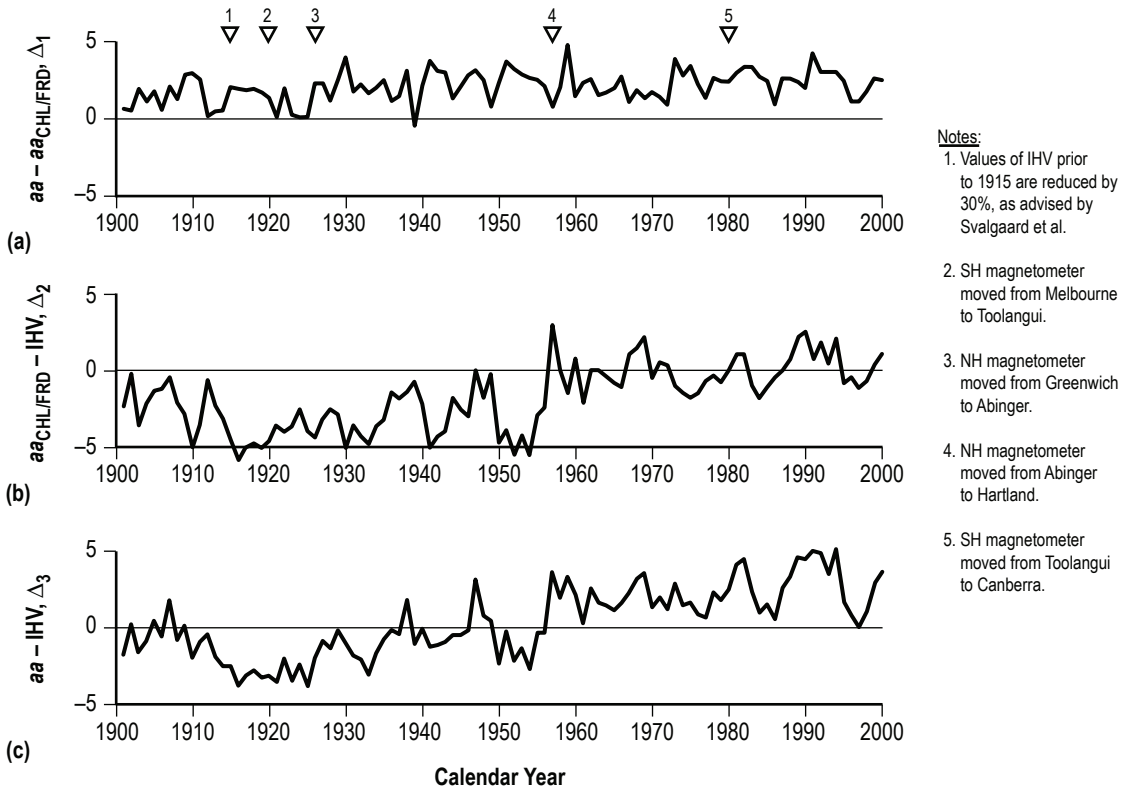

Figure 8. Variation of selected parametric differences, 1901–2000. See text for details.

Figure 8 shows the differences $aa - aa_{CHL/FRD}$, Δ_1 (panel (a)); $aa_{CHL/FRD} - IHV$, Δ_2 (panel (b)); and $aa - IHV$, Δ_3 (panel (c)), where *aa* is the observed *aa* index value; $aa_{CHL/FRD}$ is the derived *aa* value based on observations at Cheltenham/Fredericksburg during the two 3-hr periods between 0 and 6 hr UT (which represented the observed or proxy *aa* index in the Svalgaard, Cliver, and Le Sager study[19]), and IHV is the reconstructed *aa* value, these latter two values taken from Svalgaard, Cliver, and Le Sager. Across the top of the chart are time ticks 1–5, corresponding to the notes given to the right of the figure. For example, note 1 says that values of IHV prior to 1915 are reduced 30 percent, as advised in Svalgaard, Cliver, and Le Sager; note 2 states that the Southern Hemisphere (SH) magnetometer was moved from Melbourne, Australia, to Toolangui, Australia, and so forth. Today, the NH magnetometer is located at Hartland, England, and the SH magnetometer is located at Canberra, Australia. These stations are now determining the official *aa* index.

Inspection of figure 8 reveals that each of the differences appears to be relatively stable from 1957 onward, averaging about 2.3 for Δ_1, 0.1 for Δ_2, and 2.3 for Δ_3. For the earlier portion of the record, 1901–1956, Δ_1 is found to average about 1.8, Δ_2 about –3.1, and Δ_3 about –1.3. The differences of the means, especially for Δ_2 and Δ_3, are found to be statistically significant. Hence, an offset-correction appears to be needed for the earlier interval (1901–1956), one being about 3 for Δ_2 and about 3.6 for Δ_3.

Figure 9 repeats the analysis, but this time comparing *aa*, *Ap*, and IHV. Plotted are the differences *aa* – *Ap* (Δ_4) and *Ap* – IHV (Δ_5). The notes at the top of the chart refer to the notes explained in figure 8. For the interval 1957–2005, Δ_4 averages about 9.1 and Δ_5 averages about −6.7, while for the earlier interval of 1932–1956, they average, respectively, 6.8 and −7.5. So, it appears that, relative to *Ap*, the *aa* index needs to be offset-corrected by 2.3 units and, relative to IHV, *aa* should be offset-corrected by about 3.1 units (=2.3+0.8).

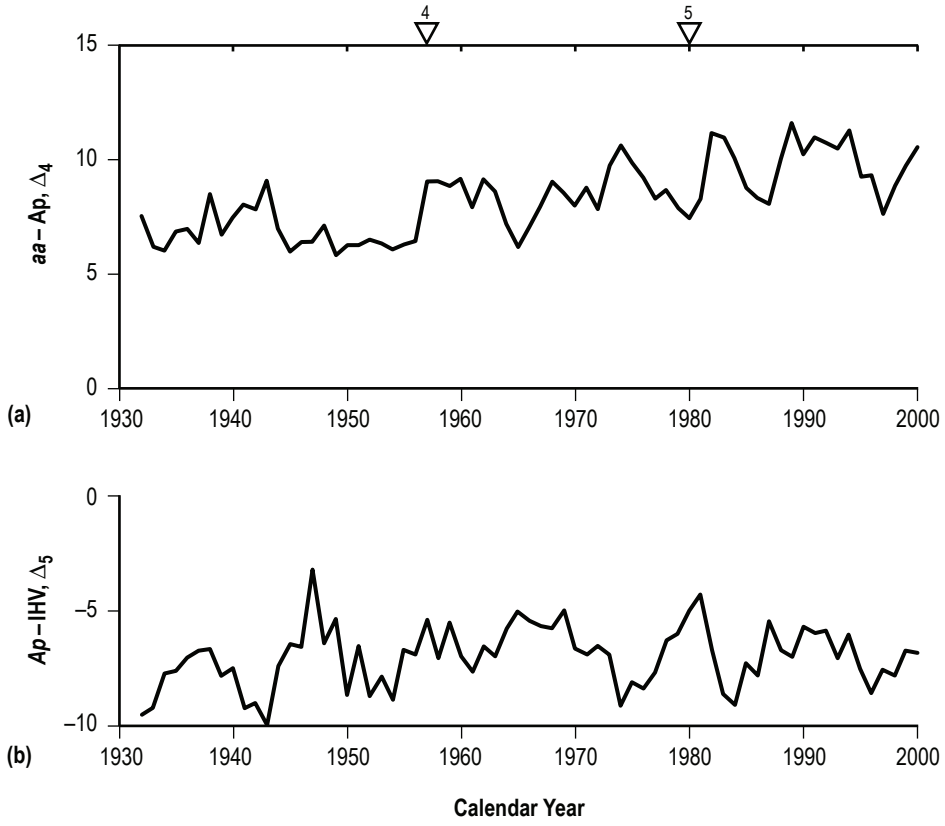

Figure 9. Variation of selected parametric differences, 1932–2000. See text for details.

Figure 10 replots *aa* versus *R*, but this time adding in an offset value of 3 to the observed values of *aa* for all values of *aa* prior to 1957. In truth, while slight offset-corrections might be attributable after each movement of the NH or SH magnetometers, for simplicity sake, a uniform correction of 3 is used to account for the general difference inferred between the earlier (prior to 1957) and later *aa* datasets.

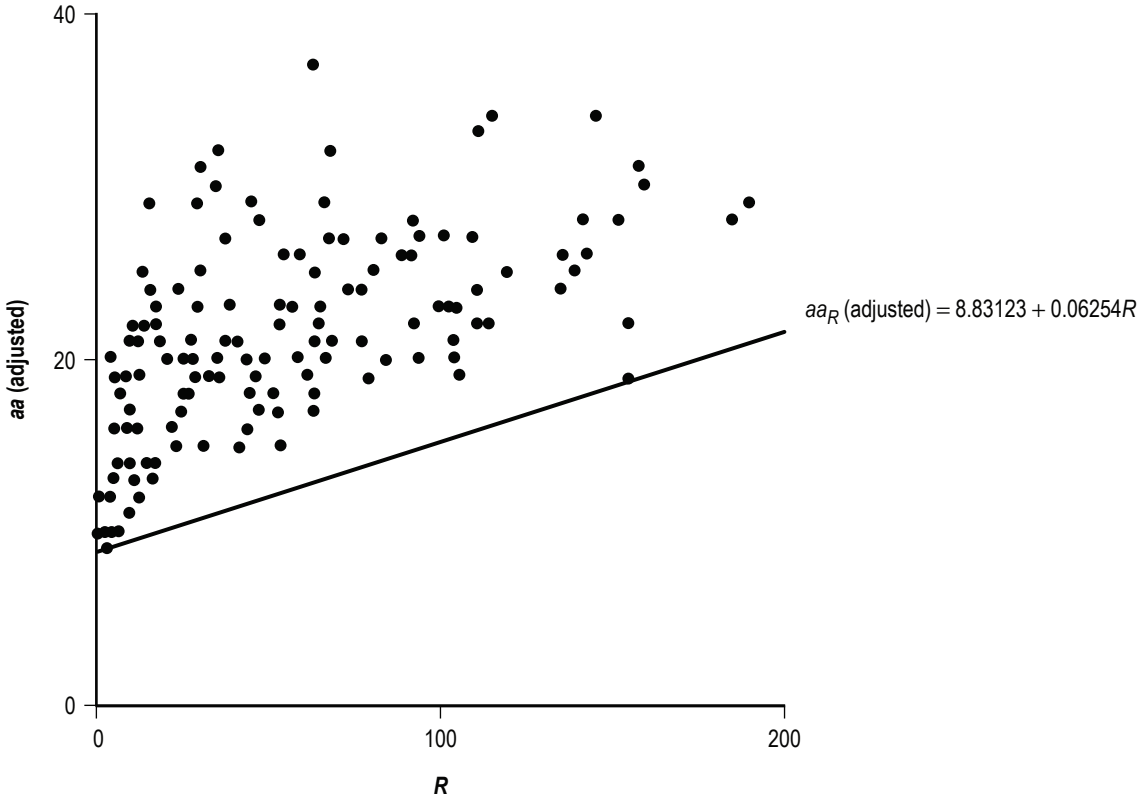

Figure 10. Scatterplot of *aa* (adjusted) versus *R*.

Figure 11 replots the aa_I component of the adjusted *aa* dataset, following the format used in figure 3. While the values of aa_I (adjusted) are shifted upward, as compared to that shown for aa_I in figure 3, there remains noticeable in both figures an increase in the value of *aa*. For example, for the interval 1868–1956, the observed (unadjusted) *aa* averaged 17.17, while for the interval 1957–2005, it averaged 23.98, an increase of nearly 40 percent. Using the adjusted *aa*, for the first interval, it averaged 20.17, as compared to 23.98 for the second interval, an increase of about 19 percent. For the same two intervals, aa_R averaged 9.69 and 12.06, nearly a 25-percent increase; aa_R (adjusted) averaged 11.79 and 13.61, an increase of about 15 percent; aa_I averaged 7.48 and 11.92, an increase of about 59 percent; and aa_I (adjusted) averaged 8.38 and 10.37, an increase of about 24 percent. Thus, the increase in geomagnetic activity appears real, being seen in both the sunspot cycle component and the interplanetary component, regardless of whether the data have been adjusted or not.

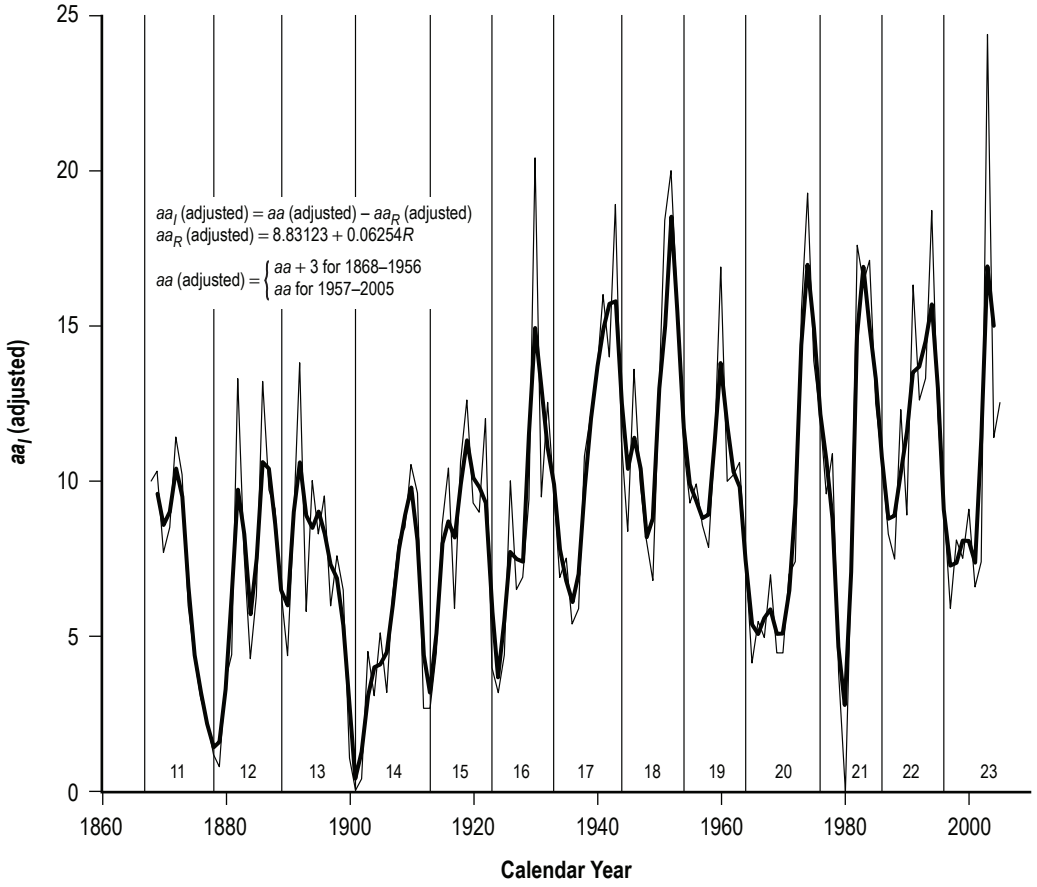

Figure 11. Variation of aa_I(adjusted). The thick line is the 2-yr moving average of the residual interplanetary component.

Figure 12 plots $R\min_2$ (cycle $n+1$) versus aa_I(adjusted) $\max_2$ (cycle n) (panel (a)), where the latter parameter refers to the maximum 2-yr moving average of the aa_I(adjusted) as plotted in figure 11, for each cycle; and $R\max_2$ (cycle $n+1$) versus aa_I(adjusted) $\max_2$ (cycle n) (panel (b)). The downward-pointing arrow gives the value of aa_I(adjusted) $\max_2$ for cycle 23, equal to 16.9. Thus, for cycle 24, the 90-percent prediction interval for $R\min_2 = 16 \pm 4.7$ and $R\max_2 = 143.2 \pm 23.2$. These values are slightly lower than what was gleaned using the observed aa (unadjusted) values. In terms of Rmin and Rm, the 90-percent prediction intervals for cycle 24 are 9.8 ± 2.9 and 8.8 ± 2.8. Similarly, in terms of Rmax and RM, the 90-percent prediction intervals for cycle 24 are 153.8 ± 24.7 and 159 ± 25.5.

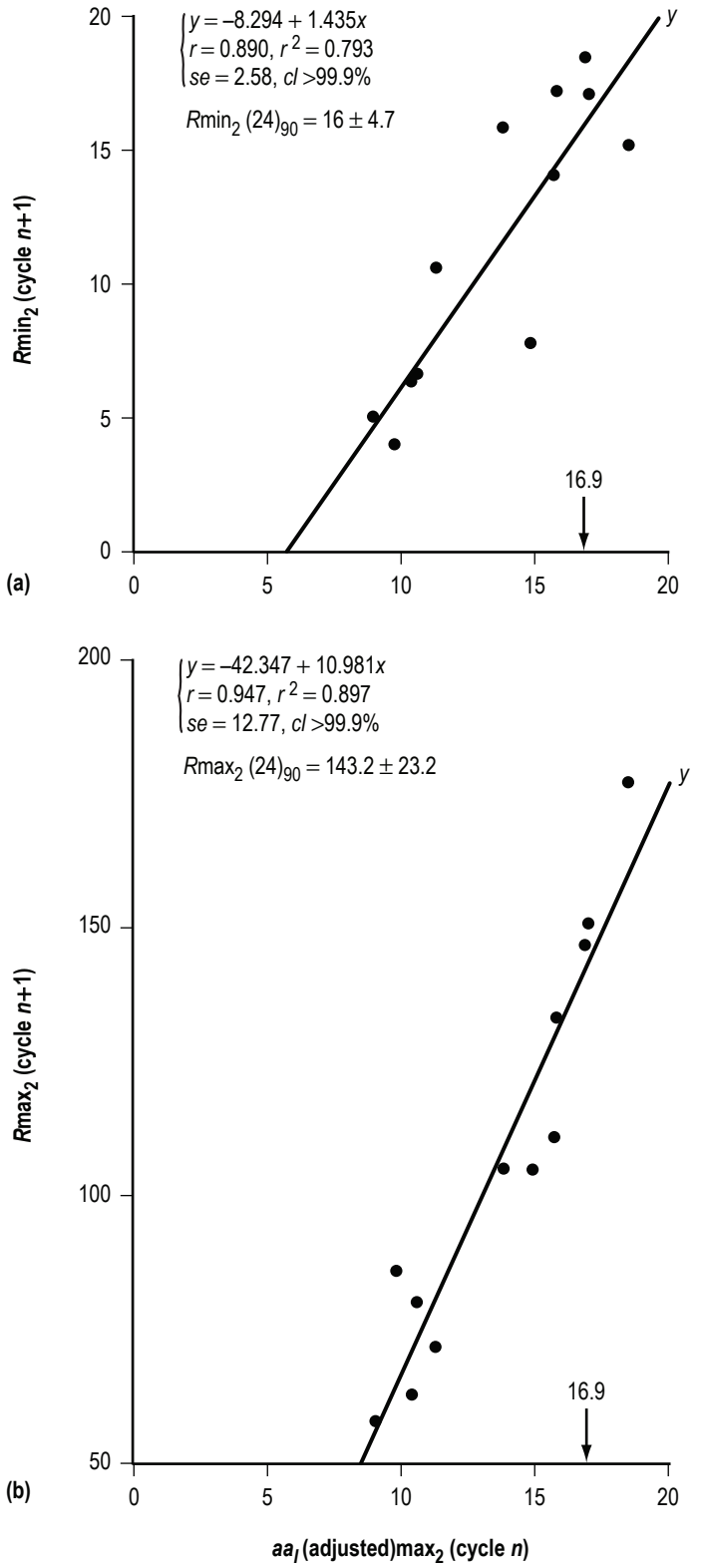

Figure 12. Scatterplots of $R\min_2$ (cycle $n+1$) versus aa_I(adjusted)$\max_2$ (cycle n) (panel (a)) and $R\max_2$ (cycle $n+1$) versus aa_I(adjusted)$\max_2$ (cycle n) (panel (b)). See text for details.

2.3 Single-Variate and Bivariate Fits Based on Parametric Minimum Values

Figure 13 displays cyclic values of *R*min (panel (a)); *R*max (panel (b)); *aa*min (panel (c)); *Ap*min (panel (d)); and NDDmin (panel (e)) for cycles 12–23. For *aa*min, *Ap*min, and NDDmin, these are the minimum values found in the vicinity of sunspot minimum (within 1 yr following sunspot minimum). This caveat is necessary because cycle 21 actually had lower values in 1980 during the maximum amplitude phase of the sunspot cycle, the only cycle in the entire record to have such an anomaly. Also, for *aa*min, two lines are plotted: the values based on the observed record and the values based on the adjusted record. Additionally, statistically significant regressions are given for *R*min, *R*max, and *aa*min (both observed and adjusted). For *Ap*min and NDDmin, only the mean and *sd* are given.

Figure 13 clearly shows that over the course of cycles 12–23, there has been an apparent secular rise in *R*min, *R*max, and *aa*min. On the basis of these inferred trends, one estimates the 90-percent prediction interval for each of the parameters to be $R\text{min} = 12.3 \pm 4.8$ (or $Rm = 11.2 \pm 4.6$), $R\text{max} = 167.9 \pm 55$ (or $RM = 173.3 \pm 56.5$), *aa*min (observed) $= 20.6 \pm 4.6$, and *aa*min (adjusted) $= 20.4 \pm 5.2$.

Figure 14 displays single-variate scatterplots of *R*max versus *R*min (panel (a)); *aa*min (panel (b)); *Ap*min (panel (c)); and NDDmin (panel (d)). Thus, observation of the minimum values of these parameters allows (at least for *aa*min, *Ap*min, and NDDmin) for the prediction of *R*max for the ongoing sunspot cycle some 2–3 yr in advance. (Although neither plot of *R*max versus *R*min is statistically significant, that based on cycles 12–23 or that based on cycles 17–23, the regressions are shown because they will be used in the next figure as part of a bivariate fit.)

From figure 14, it should be obvious that, if cycle 24 has an *aa*min of about 20, as suggested by the linear secular trend, then, clearly, one should expect an *R*max of about 160 or so for cycle 24. Such a value also suggests that *Ap*min should measure about 11 and NDDmin about 25 or so. Through July 2006, *Ap* has averaged only about 7, compared to 13.6 for the year 2005, and the total number of disturbed days amounts to only 9, compared to 43 for the year 2005. Hence, either these values will substantially increase as the year progresses, especially in the fall of the year, or cycle 24's values will fall well below the means. It is interesting to note that based on a presumed repeating pattern of "below-above-above-below" observed in *Ap*min and NDDmin, one expects both *Ap*min and NDDmin to be "above" their respective means, suggesting that the latter half of 2006 might be geophysically quite active.

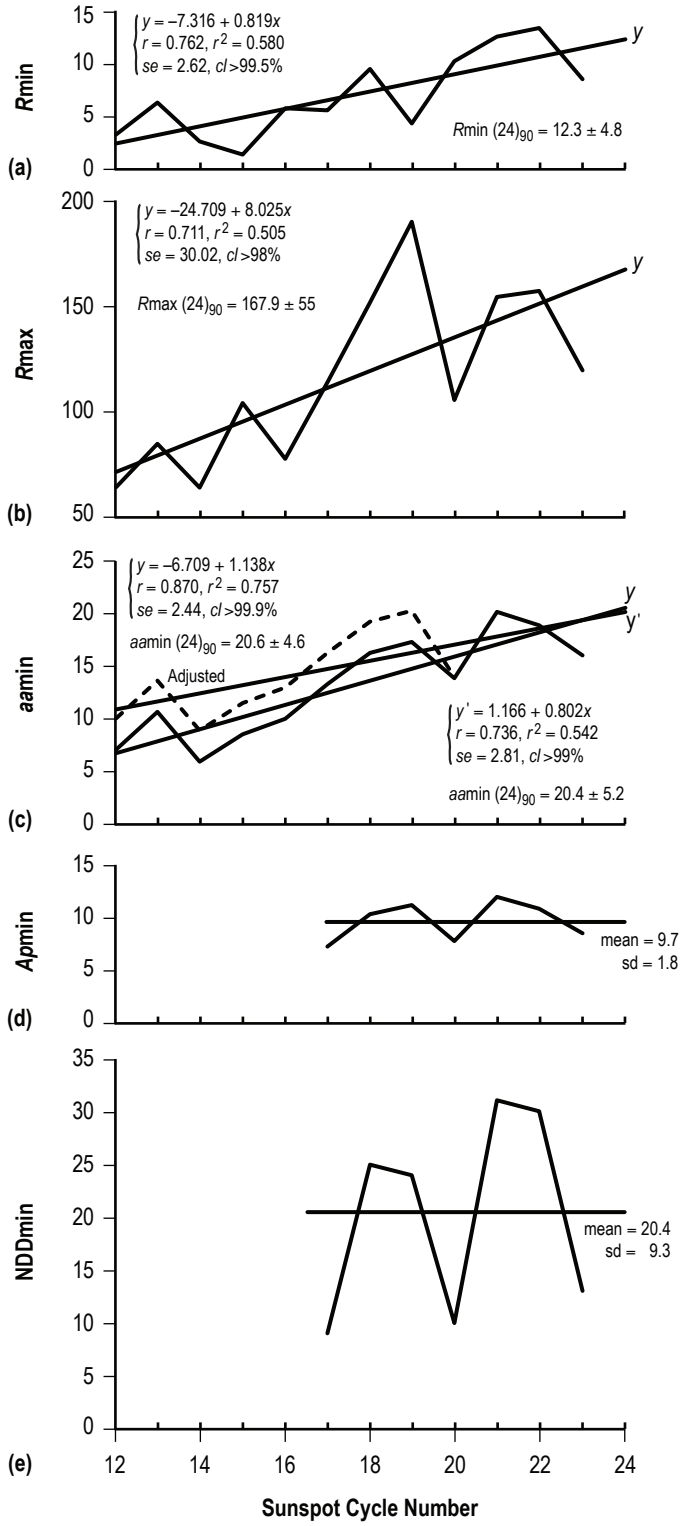

Figure 13. Cyclic variation of selected parameters. Notice the strong secular increases in *R*min, *R*max, and *aa*.

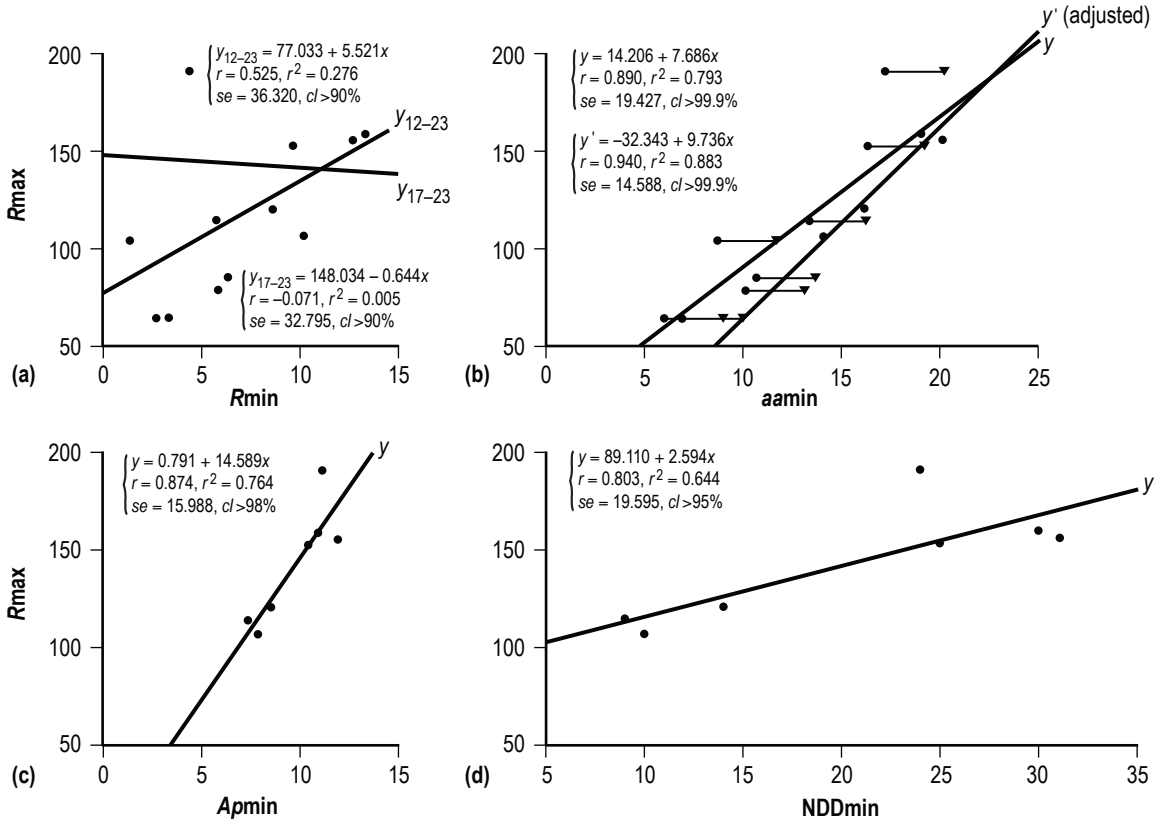

Figure 14. Scatterplots of *R*max versus selected minimum values of the parameters.

Figure 15 shows scatterplots of *R*max (observed) versus *R*max (predicted) on the basis of specific bivariate fits, where bivariate fit 1 (bv_1) is based on *R*min and *aa*min (panel (a)); bv_2 on *R*min and *aa*min (adjusted) (panel (b)); bv_3 on *R*min and *Ap*min (panel (c)); and bv_4 on *R*min and NDDmin (panel (d)). For the various fits, the one having the smallest standard error of estimate is bv_4. Thus, once *R*min and NDDmin are observed for cycle 24 (perhaps in 2007 or 2008), an alternate means for predicting *R*max for cycle 24 will be available (having a 90-percent prediction interval measuring about ±15.5 units of sunspot number).

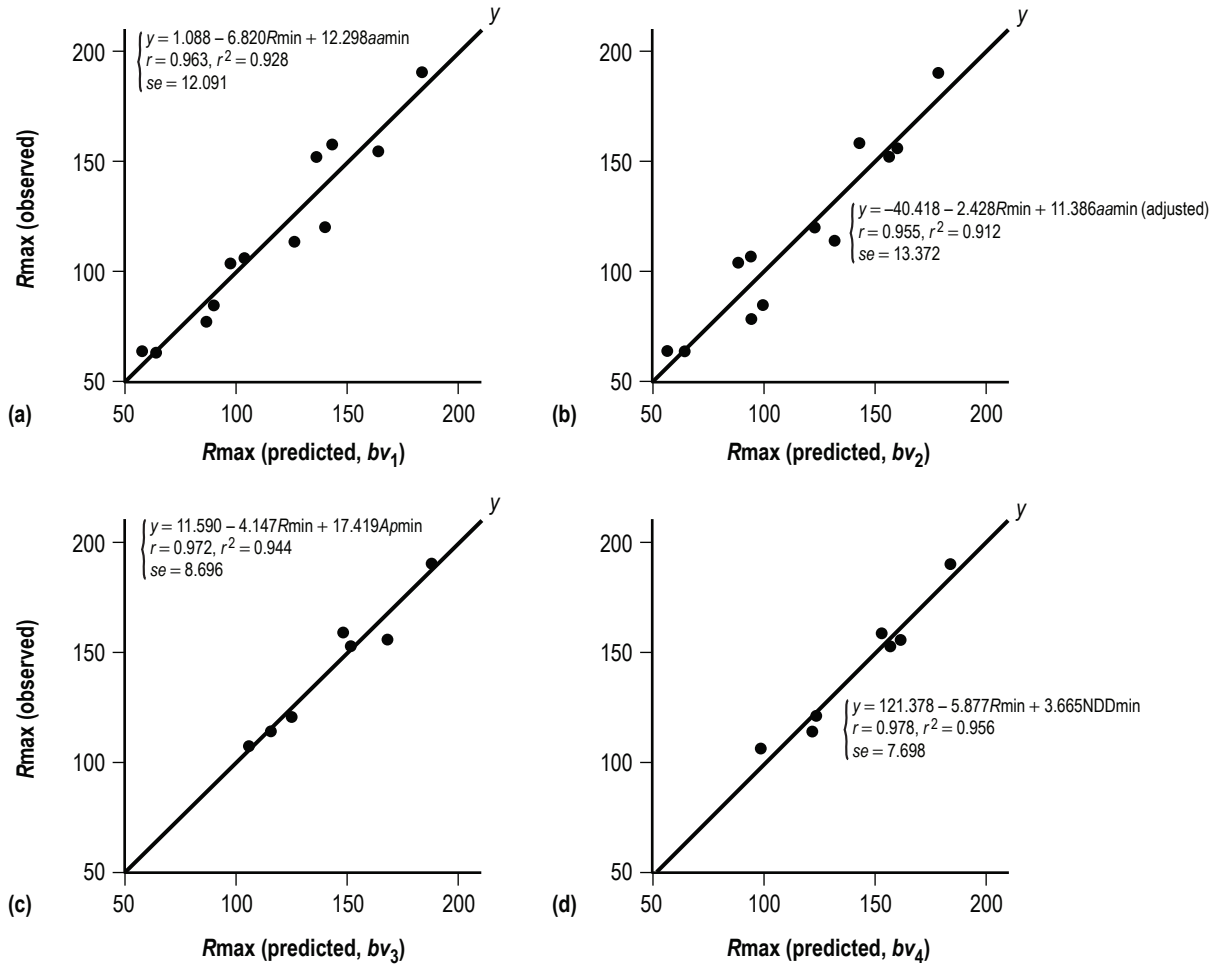

Figure 15. Scatterplots of *R*max (observed) versus selected bivariate fits. See text for details.

2.4 Cyclic Averages and Sums

Figure 16 displays cyclic averages and sums, from sunspot minimum to sunspot minimum, of <*R*> (panel (a)); <*aa*>, both the observed and adjusted (panel (b)), where the dashed line represents the adjusted values; <*Ap*> (panel (c)); <NDD> (panel (d)), where the dashed line refers to ΣNDD; and <NSSC> (panel (e)), where the dashed line refers to ΣNSSC. (<*R*> for cycle 11 excludes the year 1867 value of *R* and all parameters for cycle 23 exclude the year 2006 values.)

For <*R*>, <*aa*>, <*aa*>(adjusted), <NSSC>, and ΣNSSC, all display statistically significant upward linear secular trends, given by the regression equations. Thus, on the basis of the inferred trends, the 90-percent prediction interval of the parameters for cycle 24 is <*R*> = 82.4 ± 29.5, <*aa*> = 26.5 ± 4, <*aa*>(adjusted) = 26.2 ± 4.2, <NSSC> = 35.2 ± 6.1, and ΣNSSC = 358 ± 62. Also, because of the presumed "below-above-above-below" pattern, one expects <*Ap*> to be above 14.8, <NDD> to be above 54.4, and ΣNDD to be above 563.

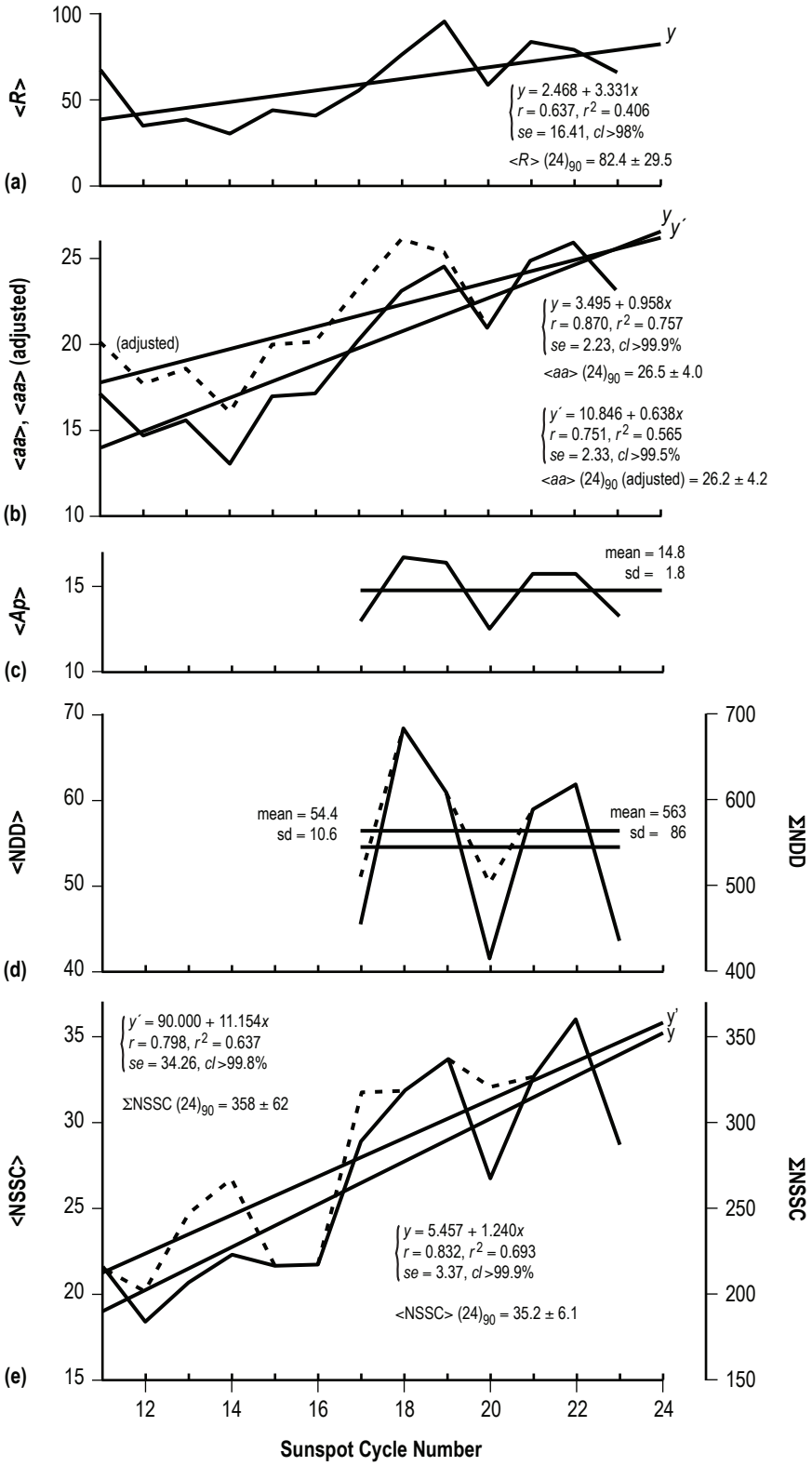

Figure 16. Variation of cyclic averages of selected parameters.

Figures 17 and 18 show comparisons of each of the parameters against *R*min (left panels) and against *R*max (right panels). All statistically significant regressions ($cl \geq 95$ percent) are identified. Hence, once *R*min has been observed for cycle 24, one can use these regressions to estimate the cyclic parametric averages (and sums). Likewise, once *R*max has occurred, one can use these regressions to estimate with greater accuracy the cyclic parametric averages (and sums). (One can also use the secular estimates to estimate *R*min and *R*max for cycle 24. The secular estimate for $<R>$ suggests that *R*min will be about 14 and *R*max about 160; the secular estimate for $<aa>$, whether adjusted or not, suggests *R*min will be about 15 and *R*max about 185; the secular estimate for <NSSC> suggests *R*min will be about 15 and *R*max about 190; and the secular estimate for ΣNSSC suggests *R*min will be about 15 and *R*max about 200.)

A peculiarity noted in figure 18 is the cyclic split seen in <NSSC> and ΣNSSC. Namely, cycles 11–16 and 17–23 appear to be grouped distinctly from each other. Such groupings reinforce the notion that cycles of late have been more robust as compared to earlier cycles. If the trend continues, then cycle 24, likewise, should be expected to be another robust cycle.[26,28–30] (Another peculiarity is the apparent "below-above-above-below" pattern noticeable in $<Ap>$, <NDD>, and ΣNDD versus *R*min or *R*max in figs. 17 and 18, which, if real, suggests above average values for cycle 24.)

Figure 19 shows the scatterplot of yearly counts of NSSC versus *R*. Plainly, years of higher *R* are associated with years of higher NSSC, and vice versa, although even during periods of low *R* (near sunspot minimum), one still expects to see about 10 or more sudden storm commencements.

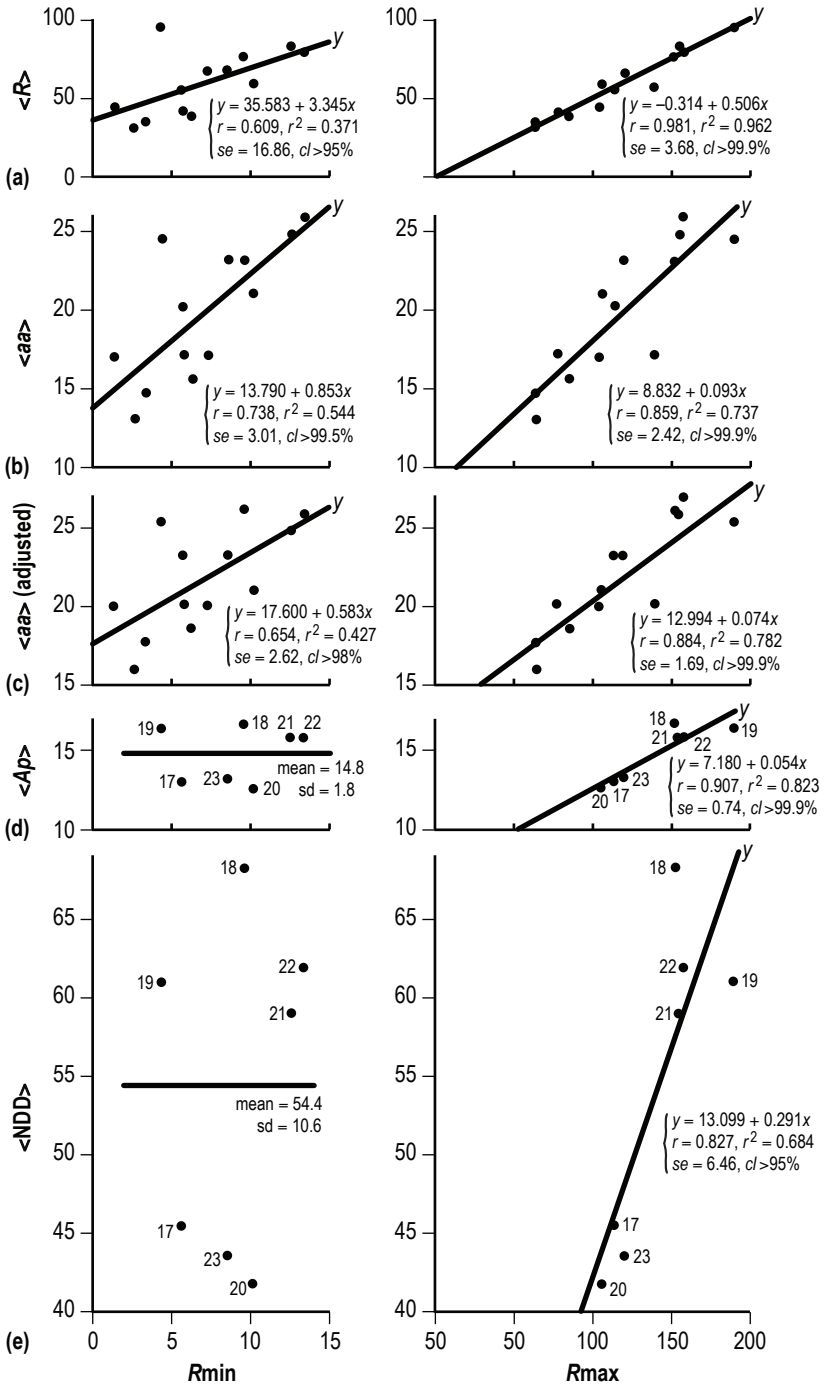

Figure 17. Scatterplots of cyclic averages of selected parameters against *R*min (left panels) and *R*max (right panels). The numbered filled circles refer to individual sunspot cycles.

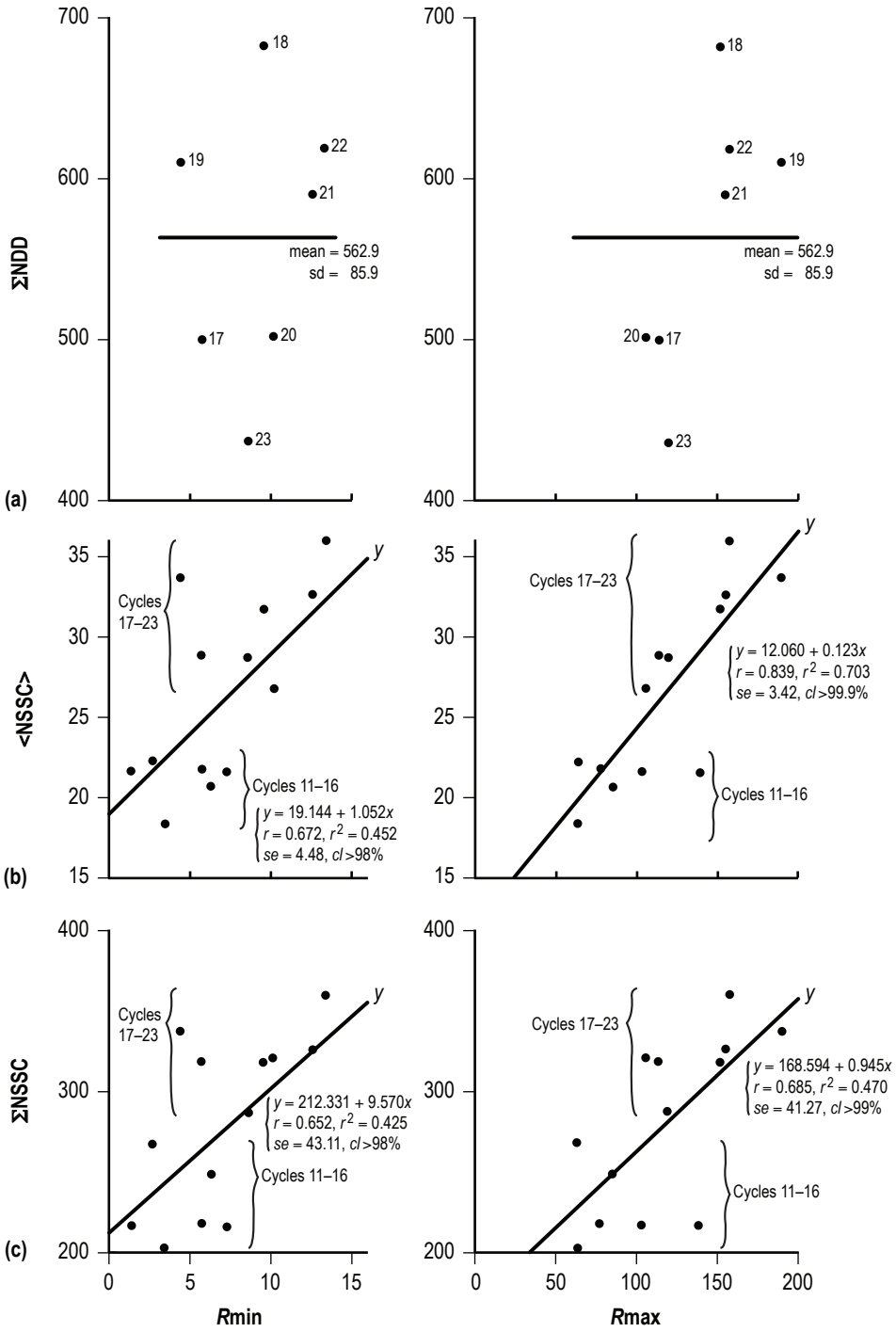

Figure 18. Scatterplots of additional cyclic averages and sums against *R*min (left panels) and *R*max (right panels).

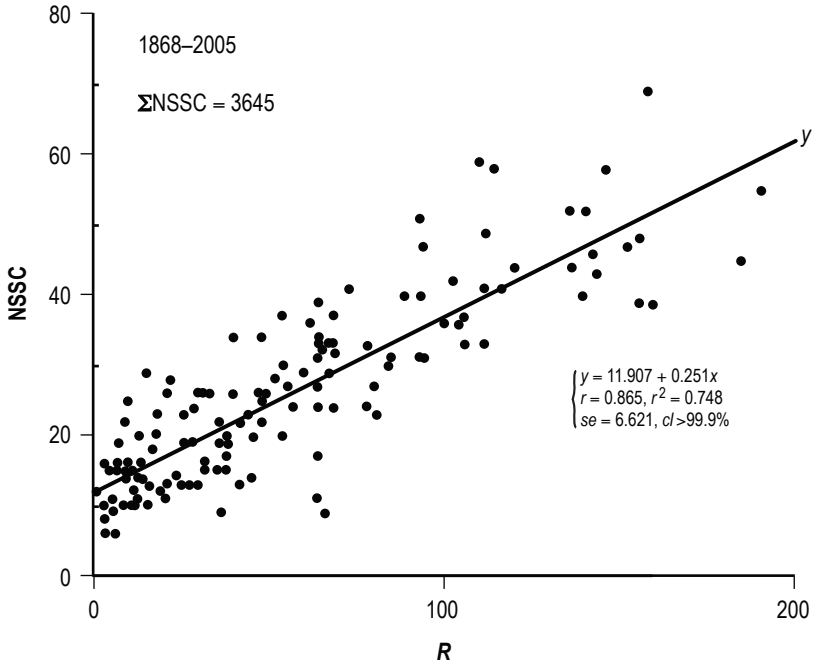

Figure 19. Scatterplot of NSSC versus *R*.

2.5 *Ap*max, ND (*Ap* ≥ 100) and ND (*Ap* ≥ 200)

Figure 20 displays the yearly *Ap*max for the interval 1932–2005. As before, the numbers at the bottom of the chart refer to sunspot cycles 17–23 and the thin vertical lines refer to the epochs of sunspot minimum for each cycle. Noticeable is that all cycles have two or more peaks of activity, with the largest *Ap*max values usually occurring after *R*max (two exceptions: cycles 18 and 22). Also, all cycles have peak values in excess of $Ap = 100$ and all but one (cycle 20) had peak values exceeding $Ap = 200$, with the highest *Ap*max (= 280) occurring in cycle 19 in November 1960 (after its *R*max). For cycle 23, its highest *Ap*max occurred in October 2003 (= 204), the sixth highest value on record.

Figure 21 depicts the scatterplot of *Ap*max versus *R*. Although there is a statistically significant positive correlation between the parameters, associating higher (lower) *Ap*max with higher (lower) *R*, one clearly sees that even when the sunspot cycle is near solar minimum there is still opportunity for large *Ap*. For example, for the 15 yr when $R < 20$, *Ap*max spanned 38 (cycle 23) to 202 (cycle 22), with one-third of the years having *Ap*max ≥ 100.

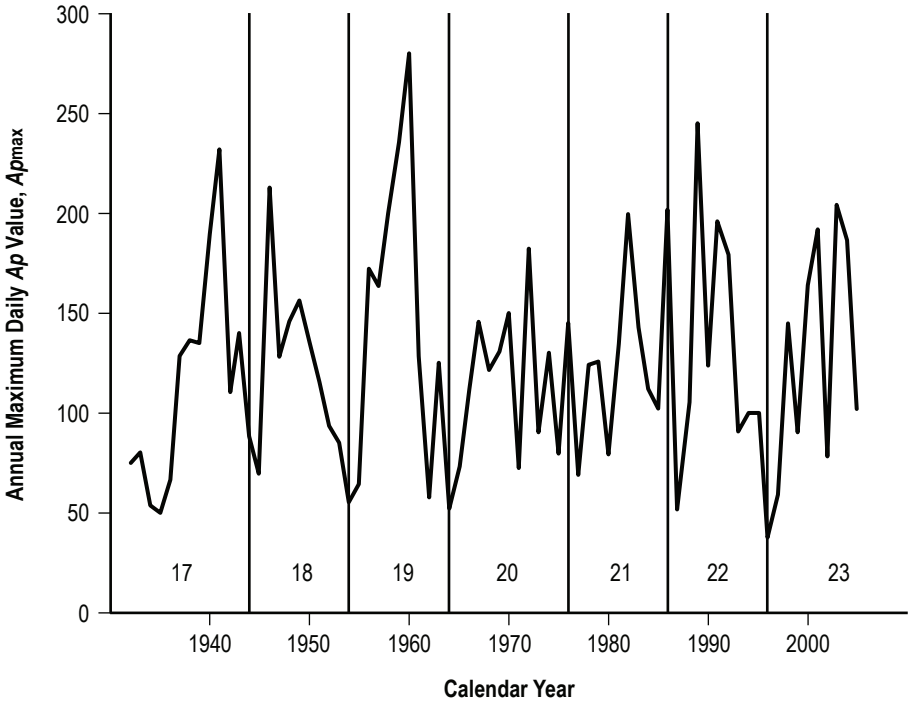

Figure 20. Variation of the annual maximum daily *Ap* value, *Ap*max.

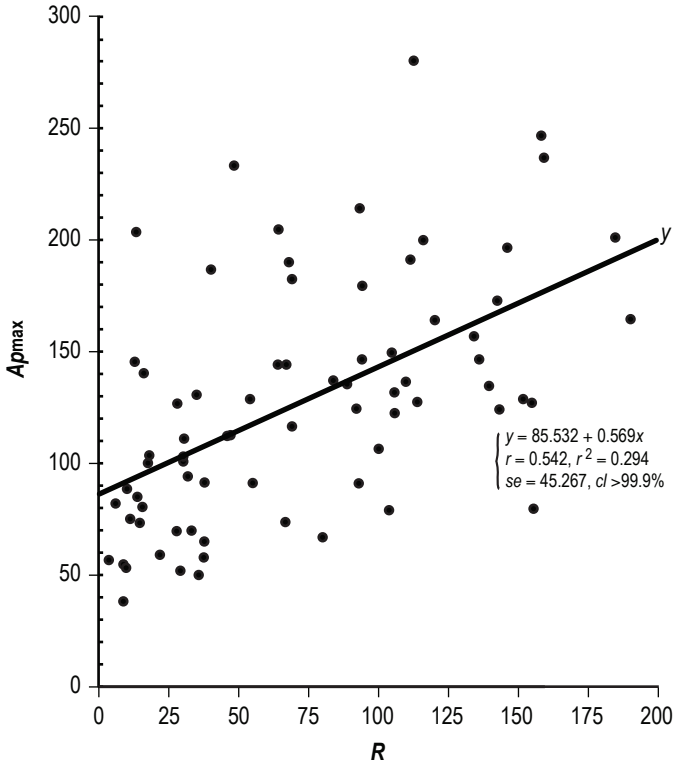

Figure 21. Scatterplot of *Ap*max versus *R*.

Figure 22 displays the scatterplot of *Ap*max versus *Ap*. Plainly, higher (lower) *Ap*max associates with higher (lower) *Ap* and the association is stronger ($r = 0.67$) than is found for R ($r = 0.54$). For $Ap < 10$, as yet, there has never been an $Ap\text{max} \geq 100$. (82 has been the largest value of *Ap*max for $Ap < 10$.)

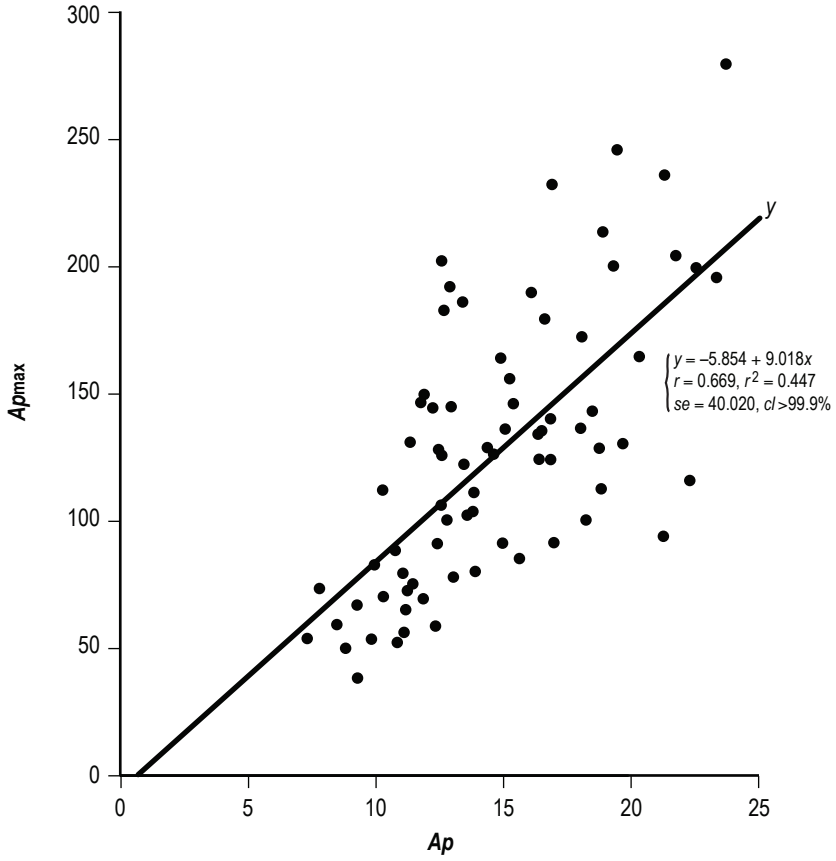

Figure 22. Scatterplot of *Ap*max versus *Ap*.

Figure 23 shows the frequency of occurrence for *E*(*Ap*max), defined here as the epoch of *Ap*max occurrence, during the year. Apparent is a semi-annual variation of the geomagnetic field, with two prominent peaks near the equinoxes and minima near the solstices.[31]

Figure 24 gives the frequency of occurrence of *E*(*Ap*max) relative to *E*(*R*max), defined here as the epoch of sunspot maximum occurrence, for cycles 17–23. Most of the cycles have their *Ap*max value 3 to 4 years after *E*(*R*max), as has previously been noted.

Figure 25 displays the cyclic variation of *Ap*max (panel (a)), and ND ($Ap \geq 100$) and ND ($Ap \geq 200$) (panel (b)) for cycles 17–23. Clearly, cycle 19 has been the most geomagnetically active cycle on record, having the highest *Ap*max (=280) and the largest ND ($Ap \geq 100$) and ND ($Ap \geq 200$) (39 days and 5 days, respectively). All cycles have had at least 13 days (cycle 20) with $Ap \geq 100$, with cycle 23 experiencing 22 such days so far, including one day of $Ap \geq 200$.

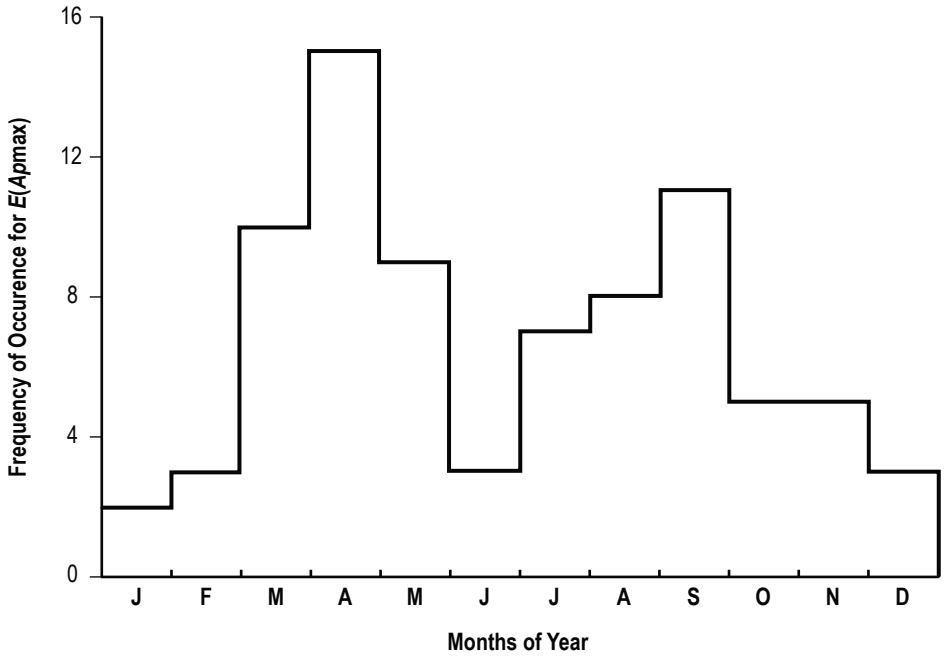

Figure 23. Semi-annual variation of *Ap*max.

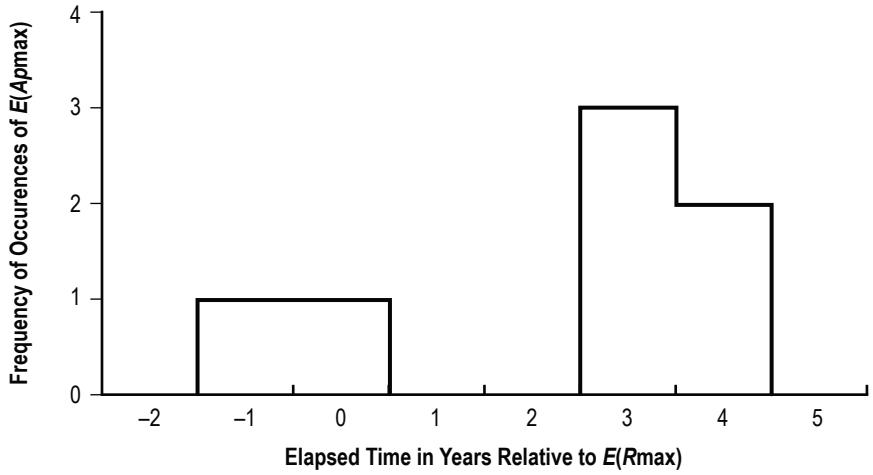

Figure 24. Histogram of the frequency of occurrences of *E*(*Ap*max) relative to the elapsed time in years relative to *E*(*R*max).

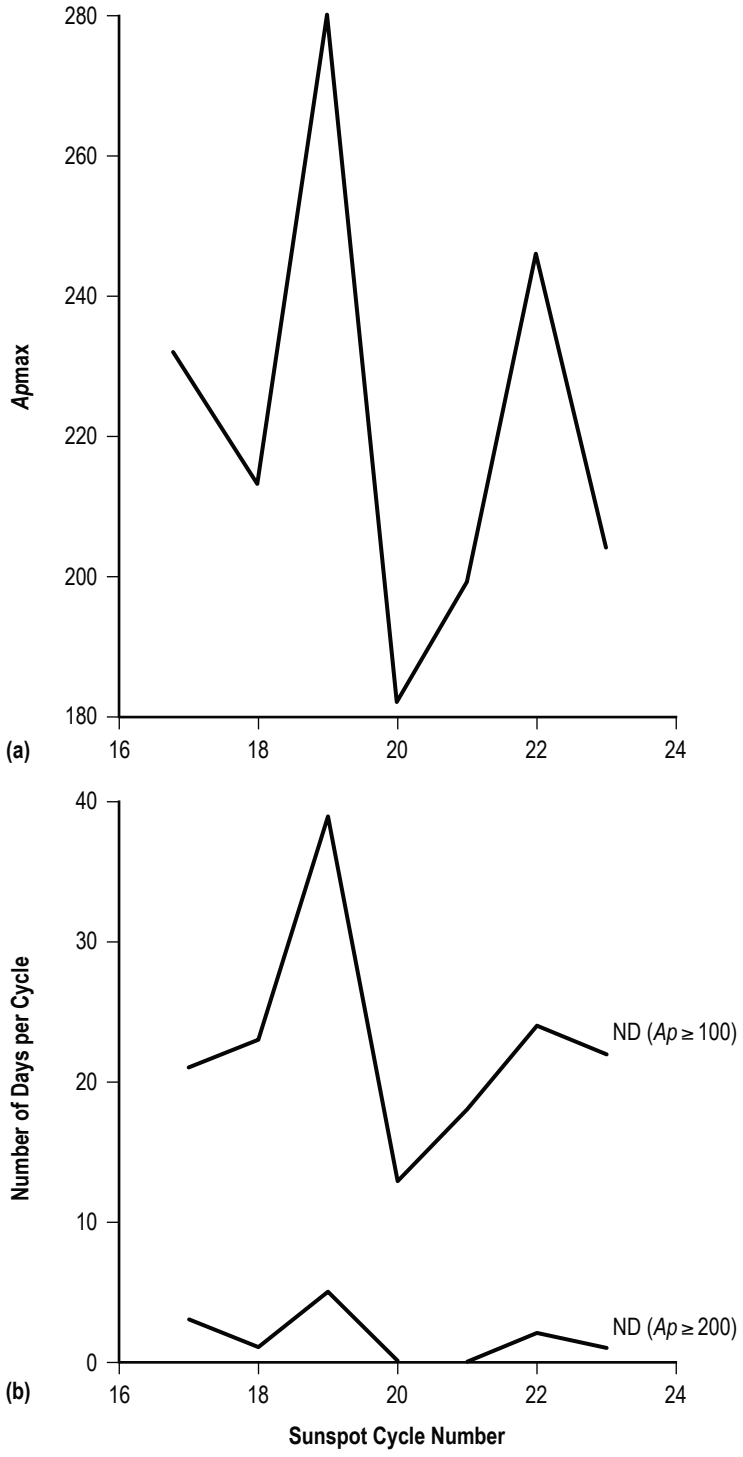

Figure 25. Cyclic variation of *Ap*max (panel (a)) and ND ($Ap \geq 100$) and ND ($Ap \geq 200$) (panel (b)).

Figure 26 depicts scatterplots of *Ap*max versus *R*min (panel (a)); *Ap*max versus *R*max (panel (b)); ND (*Ap* ≥ 100) versus *R*min (panel (c)); and ND (*Ap* ≥ 100) versus *R*max (panel (d)). Of the plots, only the latter is found to show a statistically significant positive linear regression. Thus, given the size of an ongoing sunspot cycle, one can crudely estimate the number of days during that cycle when *Ap* ≥ 100.

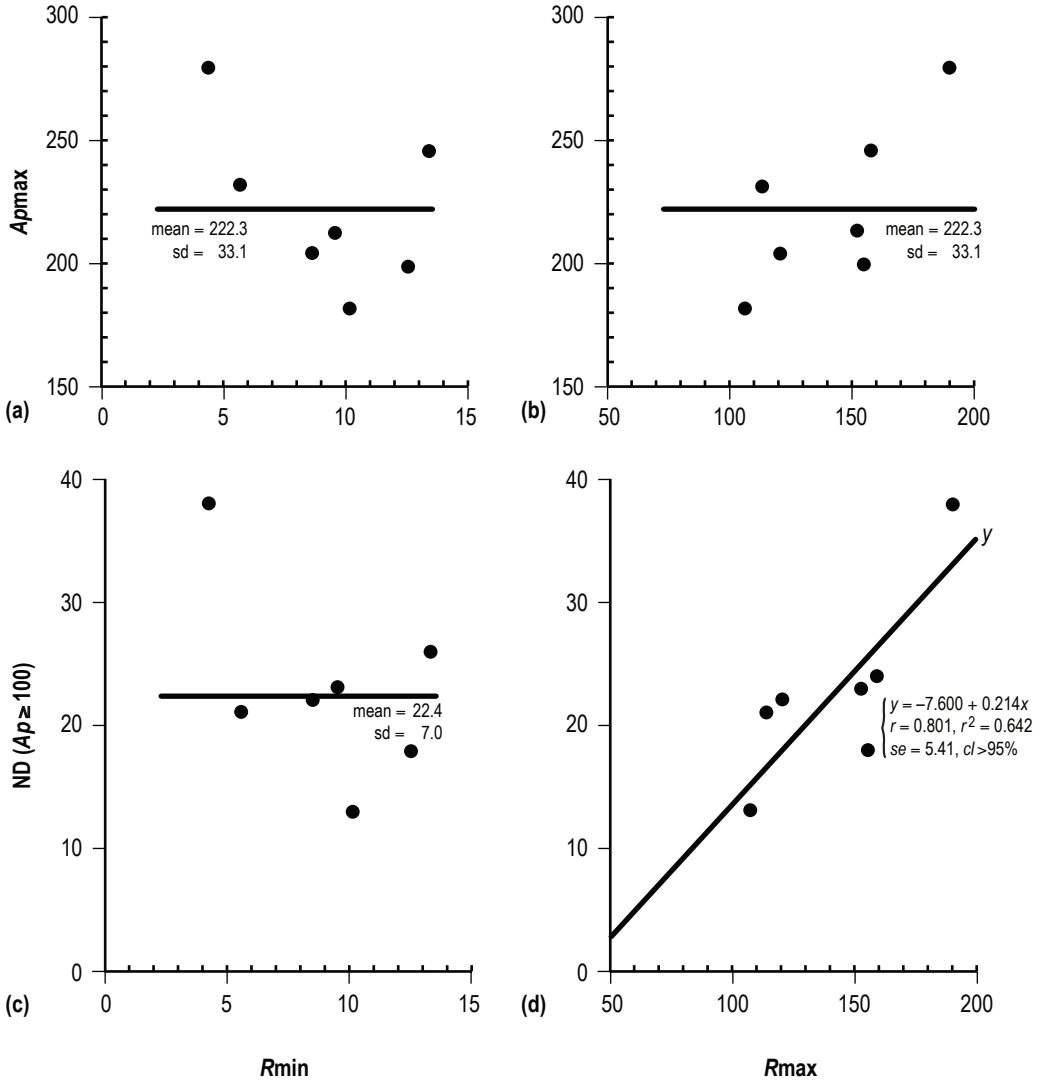

Figure 26. Scatterplots of *Ap*max versus *R*min and *R*max (panels (a) and (b), respectively) and ND (*Ap* ≥ 100) versus *R*min and *R*max (panels (c) and (d), respectively).

2.6 Estimating *Ap*, NDD, and *Ap*max Prior to 1932

Tables 1 and 2 identify single-variate (against *aa* or *aa* (adjusted)) and bivariate (*R* and *aa* or *aa* (adjusted)) regressions, respectively, for *Ap*, NDD, and *Ap*max for the interval 1932–2005. All regressions are highly statistically significant and might prove useful for determining estimates of *Ap*, NDD, and *Ap*max for the earlier interval 1868–1931. It should be noted that the bivariate fits offer no significant improvement over the single-variate fits based on *aa* or *aa* (adjusted) alone.

Table 1. Selected single-variate regressions for 1932–2005 ($n = 74$).

Correlation	r	r^2	se	cl (%)
$Ap = -2.906 + 0.761aa$	0.947	0.896	1.32	>99.9
$Ap = -4.806 + 0.808aa$ (adjusted)	0.970	0.942	0.99	>99.9
NDD = $-63.375 + 5.078aa$	0.926	0.857	10.32	>99.9
NDD = $-77.194 + 5.438aa$ (adjusted)	0.957	0.916	7.91	>99.9
Apmax = $-37.966 + 7.121aa$	0.657	0.431	40.59	>99.9
Apmax = $-47.403 + 7.213aa$ (adjusted)	0.642	0.412	41.26	>99.9

Table 2. Selected bivariate regressions for 1932–2005 ($n = 74$).

Correlation	$R_{Y.12}$	$R^2_{Y.12}$	$S_{Y.12}$
$Ap = -2.684 + 0.733aa + 0.006R$	0.948	0.900	1.27
$Ap = -4.510 + 0.775aa$ (adjusted) $+ 0.007R$	0.973	0.996	0.94
NDD = $-64.855 + 5.279aa - 0.044R$	0.929	0.863	10.15
NDD = $-78.434 + 5.600aa$ (adjusted) $- 0.037R$	0.959	0.920	7.73
Apmax = $-27.488 + 5.636aa + 0.332R$	0.716	0.512	37.85
Apmax = $-35.376 + 5.667aa$ (adjusted) $+ 0.352R$	0.711	0.506	38.11

Table 3 provides the estimates of *Ap*, NDD, and *Ap*max for 1868–1931 using the aforementioned regression fits. For simplicity, the tabular entries for NDD and *Ap*max have been rounded to the nearest whole number. Each parametric column contains two numbers: The first is the value based on the single-variate fit and the second is based on the bivariate fit. As an example, for 1868, the entries for *Ap* are 10.9 (single-variate fit) and 10.9 (bivariate fit); for *Ap* (adjusted), they are 12.3 (single-variate fit) and 12.2 (bivariate fit), and so on. To obtain the 90-percent prediction interval for the estimate, it is approximately 1.668 times the appropriate *se* for the single-variate fits and 1.668 times the appropriate $S_{Y.12}$ for the bivariate fits (given in tables 1 and 2). Thus, for *Ap*, the 1868 estimate is 10.9 ± 2.2 (single-variate fit) and 10.9 ± 1.5 (bivariate fit); for *Ap*(adjusted) it is 12.3 ± 1.7 (single-variate fit) and 12.2 ± 1.6, and so on. (The negative numbers in table 3 for NDD should be interpreted as $0 + 1.668$ *se* or $0 + 1.668$ $S_{Y.12}$, where *se* equals 10.3 or 7.9 for the single-variate fits, dependent upon using the observed or adjusted data, respectively; $S_{Y.12}$ equals 10.2 or 7.7 for the bivariate fits, dependent upon using the observed or adjusted data.

Table 3. Parametric estimates for 1868–1931.

Year	*Ap*		*Ap* (adjusted)		NDD		NDD (adjusted)		*Ap*max		*Ap*max (adjusted)	
1868	10.9	10.9	12.3	12.2	29	30	38	39	92	88	106	81
1869	12.9	13.0	14.4	14.5	42	42	52	52	110	114	124	126
1870	14.0	14.4	15.6	16.0	49	46	60	57	120	144	134	156
1871	13.3	13.6	14.8	15.1	45	43	55	53	114	130	128	142
1872	15.1	15.2	16.7	16.8	57	55	68	67	130	139	145	151
1873	12.5	12.5	13.9	13.9	39	39	49	49	106	108	120	119
1874	8.2	8.3	9.4	9.4	11	10	19	18	67	70	80	80
1875	5.6	5.6	6.7	6.6	–7	–7	0	0	42	41	55	51
1876	4.3	4.3	5.3	5.3	–15	–15	–9	–9	30	30	43	39
1877	3.9	3.9	4.8	4.8	–18	–18	–13	–13	25	27	38	36
1878	2.6	2.6	3.4	3.4	–27	–27	–22	–22	13	14	26	24
1879	2.4	2.5	3.3	3.3	–28	–28	–23	–23	12	14	25	23
1880	5.8	5.9	6.9	7.0	–5	–6	2	1	44	48	57	58
1881	7.4	7.6	8.6	8.7	6	5	13	12	59	67	80	78
1882	14.5	14.5	16.1	16.0	53	53	64	64	125	121	139	132
1883	10.4	10.5	11.8	11.8	26	25	34	34	87	92	101	103
1884	7.8	8.0	9.0	9.2	8	7	16	15	62	73	76	84
1885	8.8	8.9	10.1	10.1	15	14	23	22	72	77	85	87
1886	12.8	12.6	14.3	14.0	41	43	51	53	109	97	123	107
1887	9.6	9.4	10.9	10.6	20	21	28	29	79	69	93	79
1888	8.8	8.6	10.1	9.8	15	16	23	24	72	62	85	71
1889	6.6	6.5	7.7	7.5	0	1	7	8	51	45	64	55
1890	5.2	5.2	6.3	6.2	–9	–9	–3	–2	38	35	51	45
1891	10.0	10.0	11.4	11.2	23	23	32	32	83	80	97	91
1892	15.5	15.5	17.2	17.1	60	60	71	71	134	133	149	145
1893	10.0	10.3	11.4	11.6	23	21	32	30	83	97	97	108
1894	12.8	13.0	14.3	14.4	42	41	52	51	109	115	124	126
1895	10.9	11.0	12.2	12.3	29	28	38	37	91	96	105	107
1896	10.7	10.7	12.1	12.0	28	28	37	37	90	88	103	98
1897	7.4	7.4	8.5	8.5	5	5	13	13	58	57	72	67
1898	8.6	8.5	9.8	9.7	13	14	21	22	70	67	83	77
1899	7.1	7.0	8.2	8.1	3	3	10	11	55	50	69	60
1900	2.8	2.9	3.7	3.7	–25	–26	–20	–20	15	18	28	28
1901	1.7	1.7	2.5	2.5	–33	–33	–28	–28	5	7	18	17
1902	2.0	2.1	2.9	2.9	–30	–31	–26	–26	8	11	22	20
1903	6.1	6.2	7.2	7.2	–3	–3	4	4	47	48	60	58
1904	5.9	6.1	7.0	7.1	–5	–6	2	2	45	52	58	62
1905	8.4	8.6	9.7	9.8	12	11	20	19	68	78	82	88
1906	6.5	6.7	7.6	7.8	0	–2	7	6	50	60	64	71
1907	9.3	9.4	10.5	10.6	18	17	26	25	76	83	90	94
1908	10.0	10.1	11.4	11.3	23	23	32	32	83	84	97	95
1909	10.1	10.1	11.4	11.4	24	24	32	32	84	84	98	94

Table 3. Parametric estimates for 1868–1931 (Continued).

Year	*Ap*		*Ap* (adjusted)		NDD		NDD (adjusted)		*Ap*max		*Ap*max (adjusted)	
1910	10.4	10.3	11.8	11.5	26	27	34	35	87	77	101	87
1911	9.1	8.9	10.4	10.1	17	18	25	26	75	64	88	73
1912	3.8	3.8	4.7	4.7	–19	–19	–13	–13	25	23	38	33
1913	3.6	3.6	4.6	4.5	–20	–20	–14	–14	23	21	36	31
1914	5.4	5.4	6.4	6.3	–8	–8	–2	–1	40	37	53	47
1915	9.0	9.0	10.2	10.2	16	15	24	24	73	76	87	87
1916	12.2	12.2	13.6	13.6	37	37	47	47	103	103	117	114
1917	10.9	11.3	12.3	12.6	29	27	38	36	92	110	106	121
1918	13.5	13.6	15.0	15.0	46	45	56	56	115	120	129	132
1919	14.1	14.1	15.7	15.6	50	51	61	61	122	120	136	131
1920	10.4	10.4	11.8	11.6	26	26	34	35	87	84	101	94
1921	9.7	9.6	11.0	10.8	20	21	29	30	80	74	93	84
1922	11.3	11.1	12.7	12.4	32	33	41	42	95	83	109	93
1923	4.9	4.8	5.9	5.8	–12	–11	–5	–5	35	32	48	42
1924	4.8	4.8	5.8	5.8	–12	–12	–6	–6	34	35	47	45
1925	7.0	7.1	8.1	8.2	3	2	10	9	55	61	68	71
1926	12.2	12.2	13.6	13.6	37	37	47	47	103	105	117	116
1927	9.7	9.9	11.0	11.2	21	20	29	29	80	89	94	100
1928	10.5	10.7	11.8	12.0	26	25	35	34	87	98	101	82
1929	11.8	11.9	13.2	13.2	35	34	44	44	100	103	113	114
1930	18.8	18.4	20.6	20.2	81	84	94	96	165	145	180	156
1931	9.8	9.7	11.1	10.9	21	22	30	31	81	74	95	84

2.7 Epoch Analyses

Figure 27 shows the comparisons between yearly averages of various parametric values for cycle 23 (the filled circles) and the mean of the parametric values (the line) for cycles 11–22 (for *R*, *aa*, and NSSC) or 16–22 (*Ap*, NDD, and *Ap*max) for elapsed time in years from $E(R\text{max})$ on the basis of epoch analyses. For *R* (panel (a)), cycle 23 appears to closely mimic the behavior of the mean of cycles 11–22, suggesting, perhaps, that minimum amplitude for cycle 24 (its onset) will occur in year 7 following cycle 23's $E(R\text{max})$, this year corresponding to 2007. The proportion of cycles having $E(R\text{max})_{n+1}$ sooner than year 7 is 3/12, while the proportion having $E(R\text{max})_{n+1}$ in year 7 is 5/12 and the proportion having $E(R\text{max})_{n+1}$ in year 8 is 4/12. All cycles having $E(R\text{max})_{n+1}$ in year 8 are cycles of longer period (minimum-to-minimum duration ≥135 mo on the basis of 12-mo moving averages or smoothed monthly mean sunspot number), while all cycles having $E(R\text{max})_{n+1}$ in year 7 are cycles of shorter period (minimum-to-minimum duration ≤126 mo). Those having $E(R\text{max})_{n+1}$ in years 5 or 6 are a mixed bag, with cycles 15 and 16 being cycles of shorter period and cycle 12 being of longer period. Now, midway through 2006 (year 6), *R* has averaged only about 16. This value should become smaller as the year progresses, although it already is smaller than was seen in 5 of the past 6 cycles for comparison year 6 following $E(R\text{max})$. Also, it is nearly within the 90-percent prediction interval for *R*min based on cycles 11–22 ($R\text{min}_{90} = 7 \pm 7$). So, presently, one cannot discount that year 2006 might ultimately be the minimum amplitude year for cycle 24 marking its

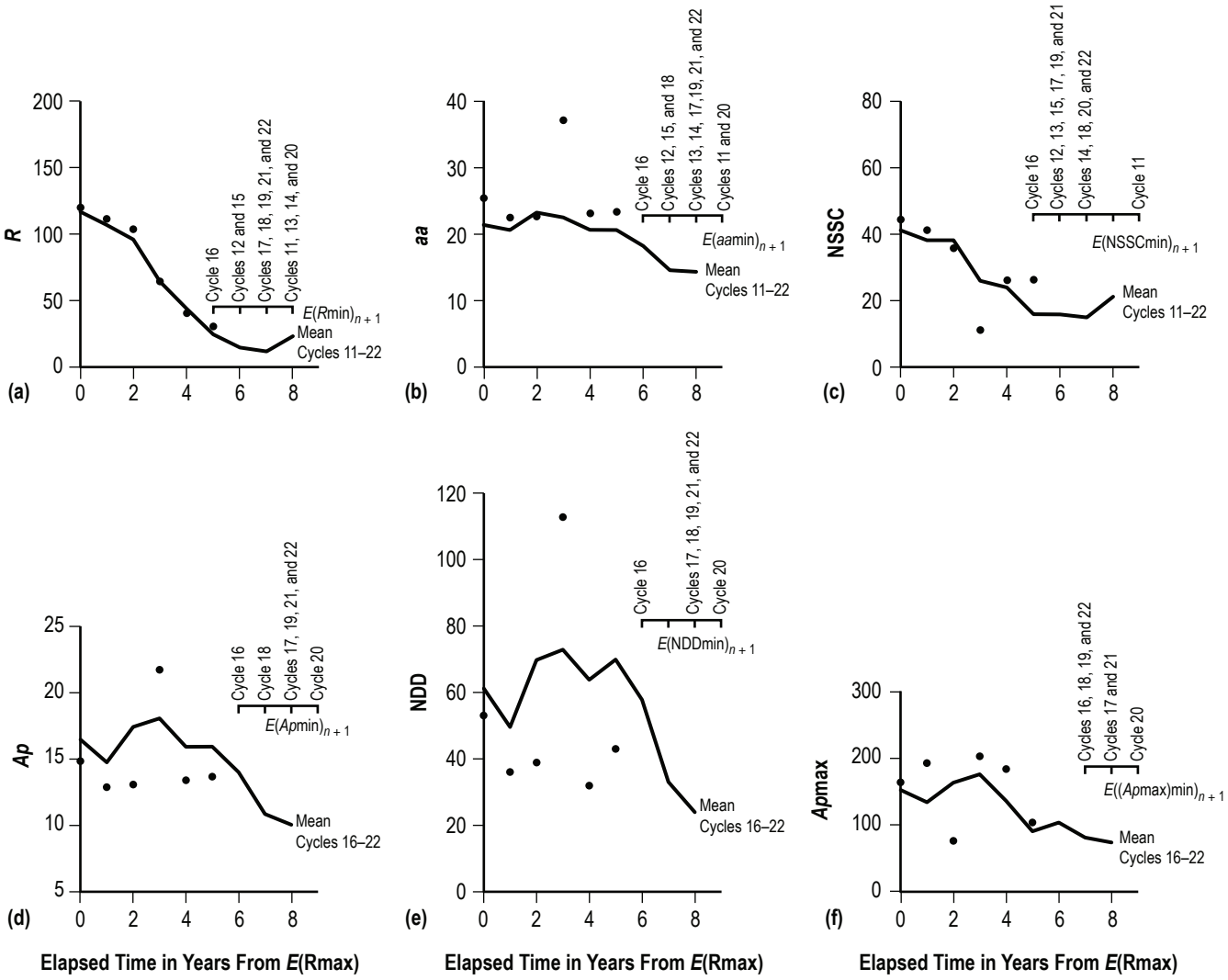

Figure 27. Comparison of cycle 23 parametric values (filled circles) and cyclic averages (cycles 11–22 or 16–22) based on epoch analyses using $E(R\text{max})$ as the temporal marker. See text for details.

onset. (It should be noted that, as yet, no new cycle spots have been seen, this being a crucial parameter for heralding the onset of a new sunspot cycle.[32–34])

For *aa* (panel (b)), it too has mimicked the mean for cycles 11–22 rather closely, except for the value at year 3 from $E(R\text{max})$ which is the highest on record, being nearly 2.5 standard deviations above the mean. The bulk of the cycles (6/12) have had $E(aa\text{min})_{n+1}$ in year 8, corresponding to 2008, suggesting that minimum amplitude occurrence for cycle 24 should be expected in 2007, since $E(aa\text{min})$ usually follows $E(R\text{min})$ by 1 yr (true for 9 of 12 cycles).

For NSSC (panel (c)), again, it too mimics the mean for cycles 11–22, except now the value for year 3 from $E(R\text{max})$ is lower than any of the past 6 cycles, but within the observed range of values (9–49) for all known cycles. Half of the sunspot cycles had $E(\text{NSSCmin})_{n+1}$ in year 6 from $E(R\text{max})$, corresponding to 2006. Since NSSC is strongly correlated ($r = 0.87$) against R (fig. 19), it may be that 2006 might turn out to be the minimum amplitude year for cycle 24. (It should be noted that cycle 21 had three consecutive years of NSSC = 20, in years 5, 6, and 7 from $E(R\text{max})$. Here, year 6 has been used as the minimum value year.)

For *Ap* (panel (d)), cycle 23's values generally have been below that of the mean for cycles 16–22, except for the peak in year 3 from $E(R\text{max})$. However, whereas the peak at year 3 for *aa* is of record value, the value at year 3 for *Ap* is only the third largest, below that which was seen for cycles 19 (23.7) and 21 (22.6).

For NDD (panel (e)), like *Ap*, the values generally have been below the mean for cycle 16–22, except for year 3 from $E(R\text{max})$. The value of 113 disturbed days, however, matches the highest ever seen, having occurred twice before in cycle 18 during years 4 and 5 from $E(R\text{max})$.

For *Ap*max (panel (f)), cycle 23's values have been above the mean for every year except year 2 from $E(R\text{max})$. Its maximum value (*Ap*max = 204) occurred in year 3.

Figure 28 is similar to figure 27, except now the comparison epoch is $E(R\text{min})_{n+1}$, meaning the epoch of the next cycle's minimum amplitude *R*min. The filled circles refer to cycle 23's parametric values, drawn presuming that onset for cycle 24 will be 2007, and the lines represent the parametric means. For R (panel (a)), the 90-percent prediction interval for R in year –1 relative to $E(R\text{min})_{n+1}$ is $R_{90} = 13.9 \pm 11.1$ and, as already been mentioned, for year 0 relative to $E(R\text{min})_{n+1}$ it is 7 ± 7. (If eventually the year 2006 is recognized as the minimum amplitude year for cycle 24, then cycle 23's parametric values must be moved 1 yr to the right in all panels.)

For *aa* (panel (b)), yearly values for cycle 23 are expected to continue to decline through $E(R\text{min})_{n+1}$ (actually to the year following the onset year for cycle 24). Certainly, if 2007 represents the minimum amplitude year for cycle 24, then $E(aa\text{min})_{n+1}$ for cycle 24 should be expected in 2008. (The proportion of cycles having $E(aa\text{min})$ in the year following $E(R\text{min})$ is 9/12.)

For NSSC (panel (c)), all yearly values for cycle 23 are above the mean, except for year –4 (2003). Its value (NSSC = 11) is more than two standard deviations below the mean and is outside the range of previously observed cycles, 14 – 49. On the other hand, one should note the sharp decrease in the mean at year –3. Should the low value of NSSC for the year 2003 be better associated with year –3 rather than –4, this might be an indication that the minimum amplitude year for cycle 24 is 2006 rather than 2007. Assuming that the 2003 value of NSSC is year –3, its value is now only one standard deviation below the mean and is within the range of previously observed cycles, 9–37. The proportion of cycles having $E(\text{NSSCmin})_{n+1}$ at year –1 is 4/12 and 5/12 at year 0. (If one assumes the 2003 value represents the year –3 value from $E(R\text{min})_{n+1}$, then the last filled circle, the 2005 value, occurs at year –1 from $E(R\text{min})_{n+1}$.)

For *Ap* (panel (d)), all yearly values for cycle 23 are below the mean, except for year –4 (2003). Its value (*Ap* = 21.7) is within the range of previously observed cycles, whether one presumes it to be year –4 (12.7–23.7) or year –3 (14.4–22.3). The proportion of cycles having $E(Ap\text{min})_{n+1}$ at year 1 relative to $E(R\text{min})_{n+1}$ is 5/7.

For NDD (panel (e)), all yearly values for cycle 23 are below the mean, except for year –4 (2003), which is outside the range of previously observed cycles (32–107). Its value (NDD = 113), however, is within the range of previously observed cycles for years –3 (52–113) and –2 (40–113). The proportion of cycles having $E(\text{NDDmin})_{n+1}$ at year 1 relative to $E(R\text{min})_{n+1}$ is 7/7.

For *Ap*max (panel (f)), all yearly values for cycle 23 have been above the mean, except for year –5 (2002), although it is within the range of previously observed cycles (73–236). Shifting the 2002 value (78) to year –4, however, places it outside the range of previously observed cycles (136–280). The proportion of cycles having $E((Ap\text{max})\text{min})_{n+1}$ is 3/7 for year 0 and 4/7 for year 1 relative to $E(R\text{min})_{n+1}$.

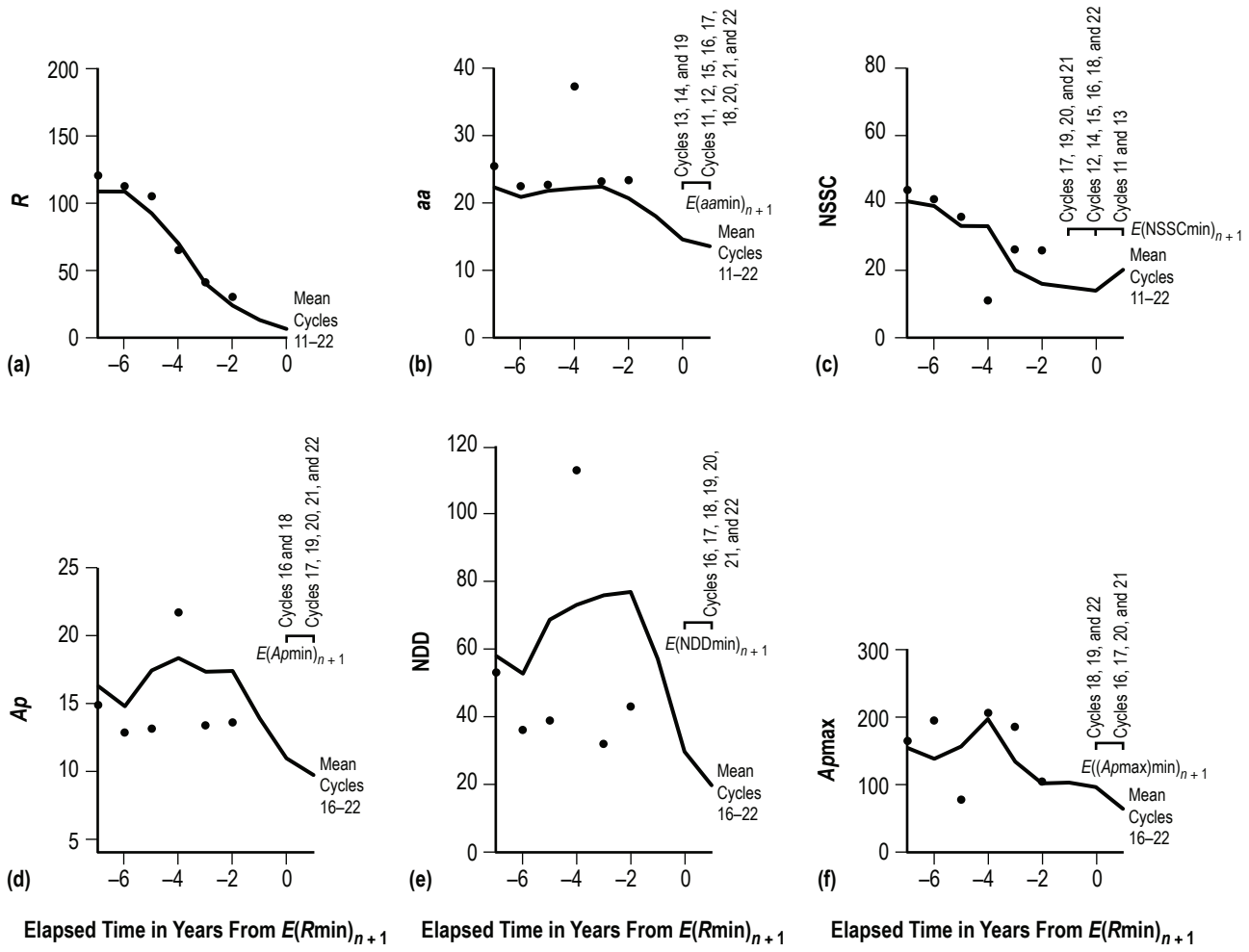

Figure 28. Comparison of cycle 23 parametric values (filled circles) and cyclic averages (cycles 11–22 or 16–22) based on epoch analyses using $E(R\text{max})_{n+1}$. See text for details.

3. CONCLUSION

This study has examined a variety of geomagnetic indices in relation to the sizes and occurrences of minimum and maximum amplitudes of sunspot cycles. The study confirms that both sunspot number and the *aa* geomagnetic index have increased over time, such that cycles of late are among the largest on record. While both sunspot number and the *aa* index is strongly correlated, there are differences between them. Namely, each sunspot cycle usually has a single peak, while the *aa* index usually has two or more peaks, often with the major peak occurring during the declining portion of the sunspot cycle.

The *aa* index was decomposed into two components—one associated directly with sunspot number *R* and the other being the residual interplanetary component due to coronal holes and the like. Plots of the residual interplanetary component, however, continue to display multiple peaks during the declining portion of the sunspot cycle, with the largest usually being the last peak just prior to sunspot minimum for the next sunspot cycle. The peaks, whether using the largest or the last-occurring peak, strongly correlate with both the minimum and maximum amplitudes of the following cycle, typically several years in advance. Unfortunately, the multiple peaks during the decline of cycle 23 present a dilemma for estimating the maximum amplitude of the next cycle. Based on the maximum value of the residual for cycle 23, cycle 24 will have $R\min_{90} = 13 \pm 4.9$ and $R\max_{90} = 183.7 \pm 46.3$, while based on the last observed residual peak, cycle 24 will have $R\min_{90} = 7.2 \pm 5$ and $R\max_{90} = 117.5 \pm 41.2$, yielding an overlap of 8.1–12.2 for *R*min and 137.4–158.7 for *R*max. The dilemma can be mitigated by applying a 2-yr moving average to the residuals, thereby yielding predictions of $R\min_{90} = 10.4 \pm 3$ and $R\max_{90} = 157.5 \pm 31.8$ for cycle 24, these annual averages equivalent to 9.4 ± 2.9 and 162.9 ± 33.5, respectively, expressed as smoothed monthly mean sunspot number.

In recent years, while studies maintain that the *aa* index has increased substantially over time, comparisons of it with the IHV index suggest that values of the *aa* index prior to 1957 might be somewhat inaccurate. In 1957, the NH magnetometer used for deriving the official *aa* index was moved from Abinger, England, to its present location in Hartland, England. The offset for the earlier *aa* values appears to measure about 3. Hence, by simply adding 3 to the observed values of *aa*, one can adjust *aa,* bringing the two disparate datasets into closer agreement. Doing so and repeating the analyses results in predictions of $R\min_{90} = 9.8 \pm 2.9$ and $R\max_{90} = 153.8 \pm 24.7$ for cycle 24, these values equivalent to 8.8 ± 2.8 and 159 ± 25.5, respectively, expressed as smoothed monthly mean sunspot number. Using the adjusted values for *aa* does not significantly alter the predictions of minimum and maximum amplitude for cycle 24, although it does reduce the uncertainty by 3 percent for *R*min and 22 percent for *R*max.

Once parametric cyclic minimum values are observed (usually, the minimum values of the geomagnetic indices occur in the year following sunspot minimum), one can use these minimum values of the geomagnetic indices to deduce with higher precision (±15.5 units of sunspot number) the size for the ongoing cycle, either on the basis of single-variate or bivariate fits (where the bivariate fits also incorporate *R*min). If the epoch of sunspot minimum is the year 2006, one should expect the minimum in the geomagnetic indices in 2007. On the other hand, if the epoch of sunspot minimum is delayed until

2007, then the minimum in the geomagnetic indices should not be expected until 2008, with sunspot maximum amplitude expected about 2–3 yr later. The best predictor of sunspot maximum amplitude after the onset of the new cycle appears to be the one incorporating both NDDmin and *R*min (bv_4), being $R\text{max}_{90} = 121.4 - 5.877\ R\text{min} + 3.665\ \text{NDDmin} \pm 15.5$ and having $r = 0.978$ and $r^2 = 0.956$, meaning that 95.6 percent of the variance can be explained by the bivariate fit.

Each of the parameters *R*min, *R*max, and *aa*min displays a secular rise over cycles 12–23, such that values for cycle 24 are $R\text{min}_{90} = 12.3 \pm 4.8$ (or $Rm_{90} = 11.2 \pm 4.6$), $R\text{max}_{90} = 167.9 \pm 55$ (or $RM_{90} = 173.3 \pm 56.5$), and $aa_{90} = 20.6 \pm 4.6$. Secular rises in *Ap*, NDD, or *Ap*max cannot be detected, owing to the brevity of these records (only about half as long as that for *aa*).

Figure 29 shows the values for seven cycle-related parameters for the interval of January 2005–July 2006, including *R*, *aa*, *Ap*, NDD, *Ap*max, NSD (the number of spotless days[28,30,35] during the month), and *d*max (the maximum daily value of sunspot number during the month) (panels (a) through (g), respectively). Plotted are the monthly means of each parameter, with the horizontal line drawn during the year 2005 representing the yearly parametric average. To the right are yearly parametric averages (90-percent probability intervals) during the sunspot minimum year. Clearly, values now being experienced in the year 2006 suggest that cycle minimum is imminent; the yearly averages for 2006 are now falling within the 90-percent probability intervals indicative of the sunspot minimum year.

In addition to the secular rises found for *R*min, *R*max, and *aa*min, cyclic averages (minimum-to-minimum) for some of the parameters are found to show statistically significant secular increases as well. For cycle 24, $\langle R \rangle_{90} = 82.4 \pm 29.5$, $\langle aa \rangle_{90} = 26.5 \pm 4$, $\langle \text{NSSC} \rangle_{90} = 35.2 \pm 6.1$, and $\Sigma\text{NSSC}_{90} = 358 \pm 62$. Also, based on a presumed inherent behavior ("below-above-above-below"), <*Ap*> will be >14.8, <NDD> > 54.4, and ΣNDD >563 for cycle 24. Furthermore, cyclic averages for cycle 24 can be deduced from cycle 24's *R*min and *R*max, once they are observed. An unexpected finding is that <NSSC> and ΣNSSC scatterplots cluster into two distinct cycle groupings: 11–16 and 17–23.

Concerning *Ap*max, all cycles are found to have had at least 1 day of $Ap\text{max} \geq 100$ and all but one (cycle 20) had at least 1 day of $Ap\text{max} \geq 200$. Opportunities for large *Ap*max remain throughout the solar cycle, including near sunspot minimum. For the 15 yr when *R* was <20, *Ap*max spanned 38 to 202, with one-third of the years having at least 1 day of $Ap\text{max} \geq 100$. $Ap\text{max} \geq 100$ has never been seen when $Ap < 10$. Once *R*max for a sunspot cycle has been observed, the number of days that $Ap\text{max} \geq 100$ can be easily estimated.

On the basis of the statistically significant regressions between *Ap*, NDD, and *Ap*max against *aa* during the interval 1932–2005, estimates can be made for the earlier interval 1868–1931.

Epoch analyses for each of the parameters suggest that sunspot minimum year for cycle 24 probably is the year 2007, although one cannot, as yet, rule out the year 2006 as the sunspot minimum year. For some of the parameters, a better fit is found using the year 2006 as the sunspot minimum year, while for others, the better fit is found using the year 2007 as the sunspot minimum year.

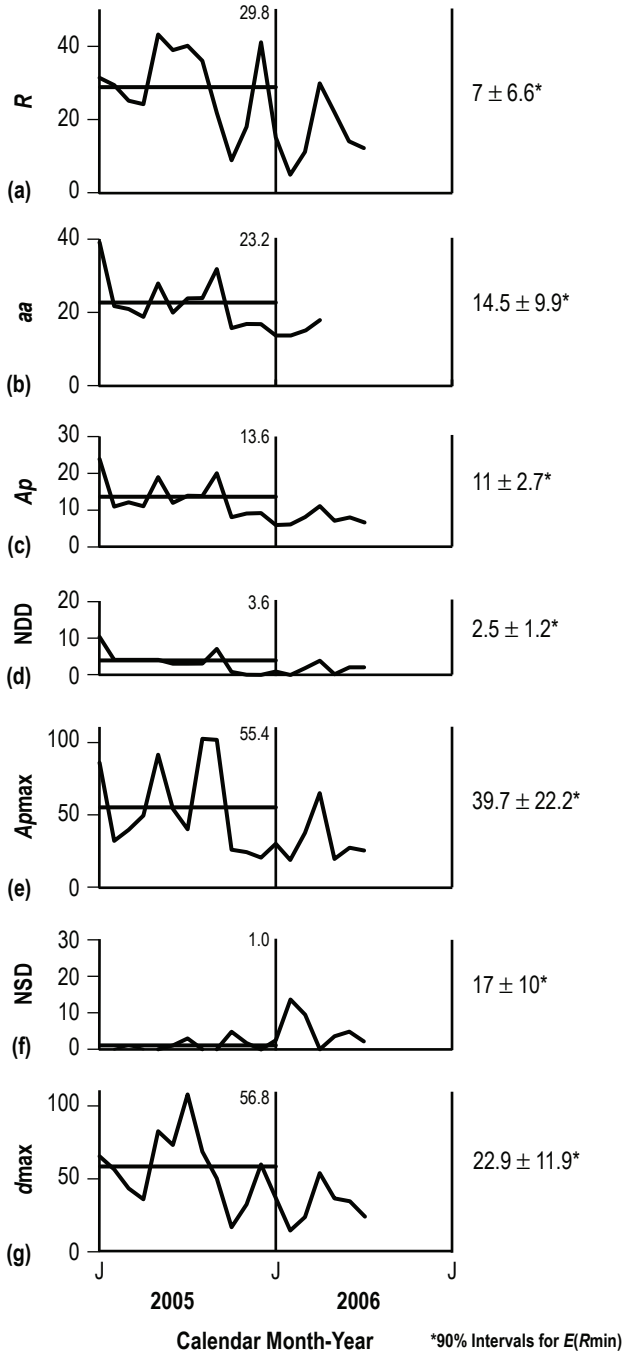

Figure 29. Parametric values for 2005 and 2006.

REFERENCES

1. Lincoln, J.V.: "I-3. Geomagnetic Indices," S. Matsushita and W.H. Campbell (eds.), *Physics of Geomagnetic Phenomena*, Vol. 1, Academic Press, New York, p. 67, 1967.

2. Patel, V.L.: "14. Solar-Terrestrial Physics," A. Bruzek and C.J. Durrant (eds.), *Illustrated Glossary for Solar and Solar-Terrestrial Physics*, Astrophysics and Space Science Library, Vol. 69, D. Reidel Publ. Co., Norwell, MA, p. 161, 1977.

3. Ohl, A.I.: "Forecast of Sunspot Maximum Number of Cycle 20," *Solice Danie*, Vol. 9, p. 84, 1966.

4. Kane, R.P.: "Maximum Sunspot Number R_z(max) in the Coming Solar Cycle No. 22—A Revised Estimate," *Solar Phys*., Vol. 122, p. 175, 1989.

5. Wilson, R.M.: "On the Level of Skill in Predicting Maximum Sunspot Number: A Comparative Study of Single Variate and Bivariate Precursor Techniques," *Solar Phys*., Vol. 125, p. 143, 1990.

6. Thompson, R.J.: "A Technique for Predicting the Amplitude of the Solar Cycle," *Solar Phys*., Vol. 148, p. 383, 1993.

7. Li, Y.: "Predictions of the Features for Sunspot Cycle 23," *Solar Phys*., Vol. 170, p. 437, 1997.

8. Bounar, K.H.; Cliver, E.W.; and Boriakoff, V.: "A Prediction of the Peak Sunspot Number for Solar Cycle 23," *Solar Phys*., Vol. 176, p. 211, 1997.

9. Jain, R.: "Prediction of the Amplitude of Sunspot Cycle 23," *Solar Phys*., Vol. 176, p. 431, 1997.

10. Kane, R.P.: "A Preliminary Estimate of the Size of the Coming Solar Cycle 23, Based on Ohl's Precursor Method," *Geophys. Res. Lett*., Vol. 24, p. 1899, 1997.

11. Lantos, P.; and Richard, O.: "On the Prediction of Maximum Amplitude for Solar Cycles Using Geomagnetic Precursors," *Solar Phys*., Vol. 182, p. 231, 1998.

12. Rangarajan, G.K.; and Barreto, L.M.: "Use of *Kp* Index of Geomagnetic Activity in the Forecast of Solar Activity," *Earth Planets Space*, Vol. 51, p. 363, 1999.

13. Hathaway, D.H.; Wilson, R.M.; and Reichmann, E.J.: "A Survey and Synthesis of Solar Cycle Prediction Techniques," *J. Geophys. Res*., Vol. 104, p. 22,375, 1999.

14. Hathaway, D.H.; and Wilson, R.M.: "Geomagnetic Activity Indicates Large Amplitude for Sunspot Cycle 24," *Geophys Res. Lett*., Vol. 33, L18101, doi:10.1029/2006GL027053, 2006.

15. Mayaud, P.-N.: "Une Mesure Planétaire d'Activité Magnétique Basée sur Deux Observatories Antipodaux," *Ann. Geophys.*, Vol. 27, p. 67, 1971.

16. Mayaud, P.-N.: "The *aa* Indices: A 100-Year Series Characterizing the Magnetic Activity," *J. Geophys. Res.*, Vol. 77, p. 6870, 1972.

17. Nevanlinna, H.; and Kataja, E.: "An Extension of the Geomagnetic Activity Index Series *aa* for Two Solar Cycles (1844 –1868)," *Geophys. Res. Lett.*, Vol. 20, p. 2703, 1993.

18. Index of ftp://ftp.ngdc.noaa.gov/STP, ftp://ftp.ngdc.noaa.gov/STP/, cited June 2006.

19. Svalgaard, L.; Cliver, E.W.; and Le Sager, P.: "IHV: A New Long-Term Geomagnetic Index," *Adv. Space Res.*, Vol. 34, p. 436, 2004.

20. Hathaway, D.H.; Wilson, R.M.; and Reichmann, E.J.: "Group Sunspot Numbers: Sunspot Cycle Characteristics," *Solar Phys.*, Vol. 211, p. 357, 2002.

21. Clilverd, M.A.; Clarke, E.; Ulich, T.; et al.: "Reconstructing the Long-Term *aa* Index," *J. Geophys. Res.*, Vol. 110, A07205, doi:10.1029/2004JA010762, 2005.

22. Wilson, R.M.; and Hathaway, D.H.: "Examination of the Armagh Observatory Annual Mean Temperature Record, 1844 –2004," *NASA/TP—2006–214434*, Marshall Space Flight Center, AL, July 2006.

23. Feynman, J.: "Geomagnetic and Solar Wind Cycles, 1900–1975," *J. Geophys. Res.*, Vol. 87, p. 6153, 1982.

24. Richardson, I.G.; Cane, H.V.; and Cliver, E.W.: "Sources of Geomagnetic Activity During Nearly Three Solar Cycles (1972–2000)," *J. Geophys. Res.*, Vol. 107, p. 1187, 2002.

25. Longley-Cook, L.H.: *Statistical Problems*, Barnes & Noble Books, New York, p. 175, 1970.

26. Dikpati, M.; de Toma, G.; and Gilman, P.A.: "Predicting the Strength of Solar Cycle 24 Using a Flux-Transport Dynamo-Based Tool," *Geophys. Res. Lett.*, Vol. 33, L05102, doi:10.1029/2005GL025221, 2006.

27. Hathaway, D.H.; and Wilson, R.M.: "What the Sunspot Record Tells Us About Space Climate," *Solar Phys.*, Vol. 224, p. 5, 2004.

28. Wilson, R.M.; and Hathaway, D.H.: "On the Relation Between Spotless Days and the Sunspot Cycle," *NASA/TP—2005–213608*, Marshall Space Flight Center, AL, January 2005.

29. Wilson, R.M.; and Hathaway, D.H.: "An Examination of Sunspot Number Rates of Growth and Decay in Relation to the Sunspot Cycle," *NASA/TP—2006–214433*, Marshall Space Flight Center, AL, June 2006.

30. Wilson, R.M.; and Hathaway, D.H.: "On the Relationship Between Spotless Days and the Sunspot Cycle: A Supplement," *NASA/TP—2006–214601*, Marshall Space Flight Center, AL, August 2006.

31. Chapman, S.; and Bartels, J.: *Geomagnetism*, Vol. 1, Oxford University Press, New York, NY, 1940.

32. Wilson, R.M.: "On the Prospect of Using Butterfly Diagrams to Predict Cycle Minimum," *Solar Phys*., Vol. 111, p. 255, 1987.

33. Wilson, R.M.; Hathaway, D.H.; and Reichmann, E.J.: "On the Behavior of the Sunspot Cycle Near Minimum," *J. Geophys. Res*., Vol. 101, p. 19,967, 1996.

34. Wilson, R.M.; Hathaway, D.H.; and Reichmann, E.J.: "An Estimate for the Size of Cycle 23 Based on Near Minimum Conditions," *J. Geophys. Res*., Vol. 103, p. 6595, 1998.

35. Wilson, R.M., "On the Use of 'First Spotless Day' as a Predictor for Sunspot Minimum," *Solar Phys*., Vol. 158, p. 197, 1995.

REPORT DOCUMENTATION PAGE

Form Approved
OMB No. 0704-0188

1. AGENCY USE ONLY *(Leave Blank)*	2. REPORT DATE	3. REPORT TYPE AND DATES COVERED
	December 2006	Technical Publication

4. TITLE AND SUBTITLE

An Examination of Selected Geomagnetic Indices in Relation to the Sunspot Cycle

5. FUNDING NUMBERS

6. AUTHORS

Robert M. Wilson and David H. Hathaway

7. PERFORMING ORGANIZATION NAME(S) AND ADDRESS(ES)

George C. Marshall Space Flight Center
Marshall Space Flight Center, AL 35812

8. PERFORMING ORGANIZATION REPORT NUMBER

M–1178

9. SPONSORING/MONITORING AGENCY NAME(S) AND ADDRESS(ES)

National Aeronautics and Space Administration
Washington, DC 20546–0001

10. SPONSORING/MONITORING AGENCY REPORT NUMBER

NASA/TP—2006–214711

11. SUPPLEMENTARY NOTES

Prepared by the Science and Exploration Research Office, Science and Mission Systems Office

12a. DISTRIBUTION/AVAILABILITY STATEMENT

Unclassified-Unlimited
Subject Category 92
Availability: NASA CASI 301–621–0390

12b. DISTRIBUTION CODE

13. ABSTRACT *(Maximum 200 words)*

Previous studies have shown geomagnetic indices to be useful for providing early estimates for the size of the following sunspot cycle several years in advance. Examined in this study are various precursor methods for predicting the minimum and maximum amplitude of the following sunspot cycle, these precursors based on the *aa* and *Ap* geomagnetic indices and the number of disturbed days (NDD), days when the daily *Ap* index equaled or exceeded 25. Also examined is the yearly peak of the daily *Ap* index (*Ap*max), the number of days when $Ap \geq 100$, cyclic averages of sunspot number *R*, *aa*, *Ap*, NDD, and the number of sudden storm commencements (NSSC), as well the cyclic sums of NDD and NSSC. The analysis yields 90-percent prediction intervals for both the minimum and maximum amplitudes for cycle 24, the next sunspot cycle. In terms of yearly averages, the best regressions give $R\text{min} = 9.8 \pm 2.9$ and $R\text{max} = 153.8 \pm 24.7$, equivalent to $Rm = 8.8 \pm 2.8$ and $RM = 159 \pm 25.5$, based on the 12-mo moving average (or smoothed monthly mean sunspot number). Hence, cycle 24 is expected to be above average in size, similar to cycles 21 and 22, producing more than 300 sudden storm commencements and more than 560 disturbed days, of which about 25 will be $Ap \geq 100$. On the basis of annual averages, the sunspot minimum year for cycle 24 will be either 2006 or 2007.

14. SUBJECT TERMS

Sun, sunspot cycle, solar cycle prediction, geomagnetic indices

15. NUMBER OF PAGES

52

16. PRICE CODE

17. SECURITY CLASSIFICATION OF REPORT	18. SECURITY CLASSIFICATION OF THIS PAGE	19. SECURITY CLASSIFICATION OF ABSTRACT	20. LIMITATION OF ABSTRACT
Unclassified	Unclassified	Unclassified	Unlimited

National Aeronautics and
Space Administration
IS20
George C. Marshall Space Flight Center
Marshall Space Flight Center, Alabama
35812